

We are IntechOpen, the world's leading publisher of Open Access books Built by scientists, for scientists

4,800

Open access books available

122,000

International authors and editors

135M

Downloads

Our authors are among the

154

Countries delivered to

TOP 1%

most cited scientists

12.2%

Contributors from top 500 universities

**WEB OF SCIENCE™**Selection of our books indexed in the Book Citation Index
in Web of Science™ Core Collection (BKCI)

Interested in publishing with us?
Contact book.department@intechopen.com

Numbers displayed above are based on latest data collected.
For more information visit www.intechopen.com



Practical Continuous-Wave Intracavity Optical Parametric Oscillators

Dr David J M Stothard
University of St. Andrews
United Kingdom

1. Introduction

The mid-infrared spectroscopic region ($\sim 1.5\text{-}5\mu\text{m}$) is one of ever increasing importance. Many hazardous, contraband or otherwise important molecules and compounds exhibit their peak rotational and vibrational absorption features over this wavelength range and so can be readily detected and identified through the use of spectroscopic techniques. There is an urgent requirement, therefore, for high spectral purity, compact and wavelength-flexible optical sources operating over this range. Laser based spectrometers operating at visible or near-infrared wavelengths offer a combination of unprecedented resolution and ease of use due to their extremely high spectral brightness and tunability. Mid-infrared laser-based spectroscopy is, however, far less developed (even though this spectral range is arguably of more scientific importance) due to a severe lack of suitable continuous-wave (cw), broadly tunable laser sources. Whilst this area has attracted intense research interest over the past decade, current state-of-the-art mid-infrared laser systems are still not poised to address this shortfall. Quantum-cascade, difference-frequency mixing techniques and lead-salt diodes produce very low output power, limited tunability, poor spatial mode quality, require liquid cryogenics, or a combination of these.



Fig. 1. The generation of long wavelength light through parametric frequency down-conversion. Here, $v_p = v_s + v_i$.

The use of nonlinear optical techniques to convert the output of laser systems operating at too short a wavelength, but otherwise exhibiting meritorious characteristics (e.g. high efficiency, robust design, etc) to the low frequency, mid-IR band of interest has received considerable interest since the invention of the laser in the early 1960s. Such nonlinear devices are called *optical parametric oscillators* (OPOs) and they operate by dividing the energy of an incoming, high energy pump photon into two lower energy photons (denoted the signal and idler); the energy (and hence, frequency) of which add up to that of the pump

Source: Advances in Optical and Photonic Devices, Book edited by: Ki Young Kim,
ISBN 978-953-7619-76-3, pp. 352, January 2010, INTECH, Croatia, downloaded from SCIYO.COM

(see Fig. 1). One of the simplest incarnations of this device is the externally-pumped, or *extra-cavity, singly-resonant OPO* (ECOPO) - (see Fig. 2(a)). Here, a nonlinear optical crystal is placed within an optical cavity exhibiting high finesse at one of the down-converted waves (most usually, the signal wave). Once pumped hard enough, the parametric gain overcomes the round-trip loss experienced by the resonant wave and the OPO reaches threshold: down-conversion from the incident pumping wave to signal and idler begins. Crucially, as the parametric process is not limited to a particular electronic or vibrational transition (as in the case of a laser), the tuning range of the down converted signal and idler waves are limited only by the transparency of the nonlinear dielectric material in which they are generated. Hence it is possible to realise devices which exhibit very broad tunability in the down-converted signal and idler waves even if the pumping laser is not itself tunable (although pump-laser tunability does enable an additional tuning mechanism).

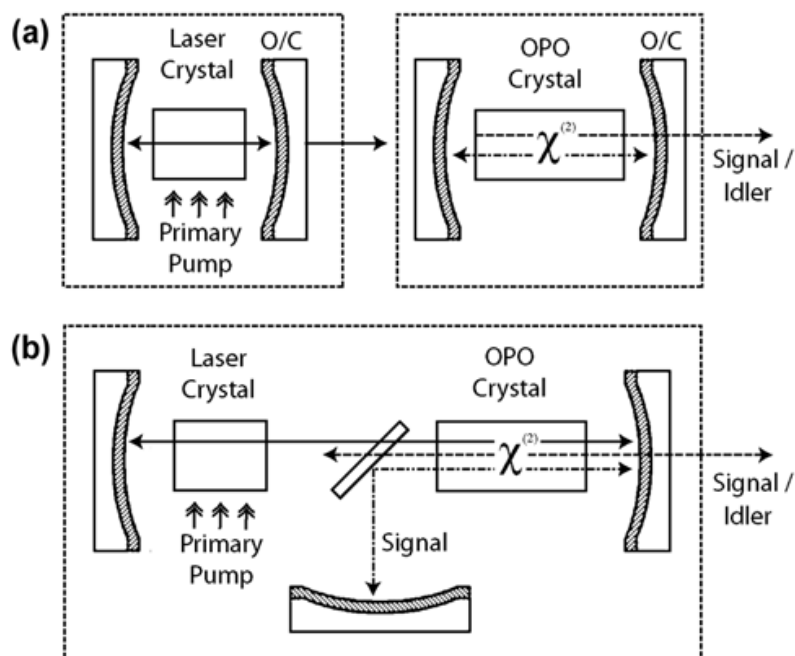


Fig. 2. Externally-pumped (a), and intracavity (b) optical parametric oscillators (ECOPO and ICOPO). Note that in both of these geometries, the optical cavity in which the nonlinear crystal resides is resonant at only one of the down-converted waves (i.e. either signal or idler).

It is the large offset pumping power needed before downconversion begins (the *threshold* pumping power) which is the main objection to the widespread implementation of the ECOPO. Before the advent of long interaction length periodically-poled nonlinear crystals exhibiting comparatively large nonlinearity-interaction length products, threshold pumping powers were on the order of many tens of watts – therefore precluding their use with all but the most powerful cw pump lasers. When one takes into account the primary pumping power required to excite the pumping laser gain medium then the overall efficiency picture of these devices looks even bleaker. This has changed with the introduction of the aforementioned periodically-poled nonlinear materials, most notably the now-ubiquitous periodically-poled LiNbO_3 (PPLN) crystal. This brought threshold pumping powers down to the 3-5W level, i.e. within the reach of moderately powered cw laser systems. Overall “wall-plug” efficiency is however still very poor, though, unless ECOPOs are operated well above ($\sim 2\text{-}3\times$) threshold (more of this on section 2.1). The highly efficient production of

multiple-watt output in the down-converted signal and idler fields is therefore perfectly possible (and indeed has been amply demonstrated (Bosenberg, Drobshoff et al. 1996)) in the ECOPO geometry *but* very poor efficiency results when the output is in the 10s-100s mW region (i.e. the device is operated closer to threshold). This is problematic as many (if not most) of the potential applications of a broadly tunable mid-IR source only require moderate power levels. In addition to this, for many industrial, medical, forensic and field uses, high efficiency, highly compact devices (i.e. battery powered, air-cooled) are a must.

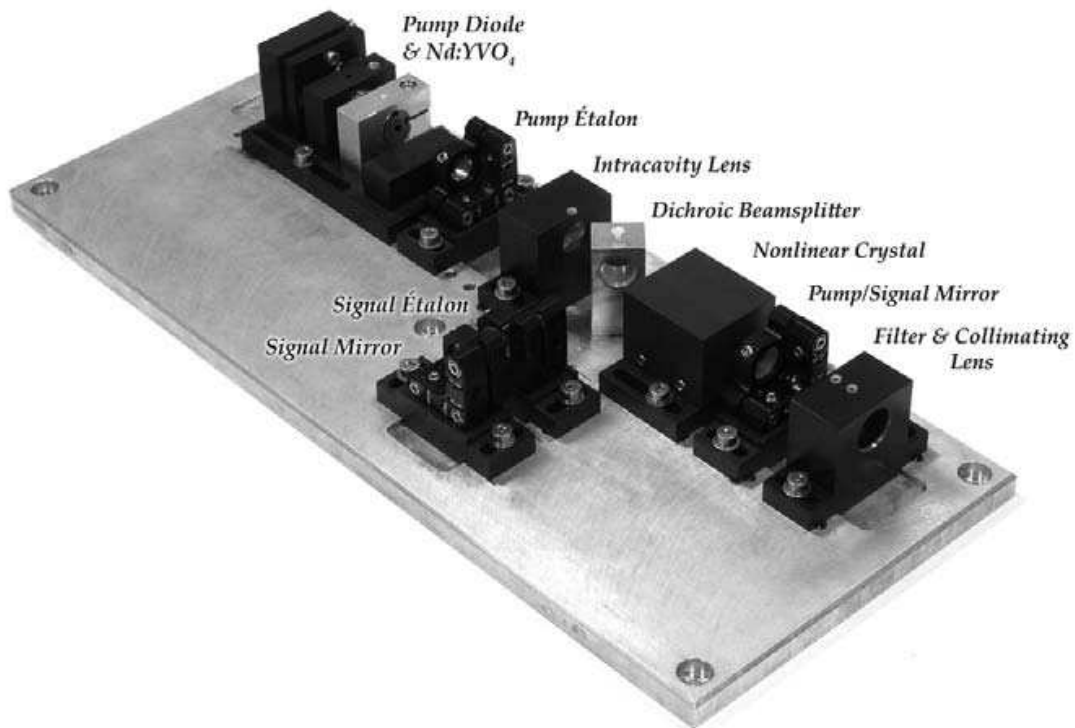


Fig. 3. A well-engineered, all solid-state miniaturised cw-ICOPO. This device consumes just ~ 10 W electrical power, can deliver >500 mW in the down-converted optical fields and requires no forced cooling. The function of the various components is discussed later in the text.

An elegant solution to this problem comes through taking advantage of the very high circulating field found within the (high-finesse) cavity of a laser. If one replaces the lasers' output coupling mirror with a high reflector, very high (10's W) circulating fields can result even when pumped at low (100's mW) levels. Placing the OPO *inside* the laser cavity (see Fig. 2(b)) then gives the parametric process access to this high field and the OPO comes to threshold at very much lower primary pumping powers than is the case with the ECOPO, thus obviating the high primary pumping power threshold requirements associated with that geometry. This, the *intracavity optical parametric oscillator* (ICOPO) enables the realisation of extremely compact, highly efficient devices which can exhibit high output powers in the down converted waves (100's mW) when pumped with only very modest (1's W) primary (i.e. diode-laser) pumping sources. An important consequence of the unprecedented down-conversion efficiency afforded by the intracavity approach, coupled with the robust operating nature of the singly-resonant design, is the possibility of realising battery / field operable systems as the need for large frame pumping lasers, forced water cooling and high cost is eliminated. A photograph of such a system is shown in Fig. 3. Here, for just 3W of primary pump power from the integrated diode laser pump module, 300mW and 150mW of

broadly tunable signal and idler power are delivered. Because of the very high efficiency exhibited by the ICOPO, no forced air or water cooling is required. The device consumed <10W electrical power, making it ideal for battery power, portable or remote operation.

From a power and efficiency point of view, then, the cw-ICOPO represents an excellent solution to the problem of inadequate spectroscopic laser-source coverage over the mid-IR range. Unfortunately, there is a particular problem associated with the intracavity approach which has to date severely hampered its widespread implementation. The practical application of very narrow linewidth (sub MHz), diode pumped ICOPOs requires continuous wave output and therein lies a serious limitation inherent in the underpinning physics of the ICOPO. This is due to the impact of the OPO upon the transient dynamics of the Neodymium-based pump lasers in which to date they have been operated. Clearly, maintaining a diode pumped, all solid-state parent laser is highly desirable and hence the majority of ICOPO research has been predicated upon the use of Neodymium (Nd) based laser gain media. Whilst exhibiting many excellent characteristics ideally suited to this technology, their long upper state lifetime (compared to the decay time of the laser and signal waves in their respective cavities) leads to unpredictable and prolonged bursts of relaxation oscillations when used in consort with the intracavity technique. Such behaviour has an unacceptable impact on the frequency and amplitude stability of the down-converted waves and has to date precluded the Nd-based CW ICOPO from having lived up to its considerable potential.

In this chapter we will explore the design criteria for the realisation of practical intracavity cw-OPO systems, with a particular emphasis on overcoming their susceptibility to the spontaneous onset of relaxation oscillations. We shall begin with a comparison between the operating characteristics of cw intracavity OPOs and their externally-pumped counterparts (without becoming bogged down in a turgid foray into nonlinear optical theory (Oshman & Harris 1968)), and the design rules which must be fulfilled in order to realise optimal operation in the intracavity regime. These rules will be applied and tested by then considering the design and realisation of a real-life system previously reported in the literature; the steps taken in order to maximise the chances of successful operation of the device will be reviewed. The discussion will then move on to the vexing problem of relaxation oscillations which occur in the intracavity context; this will be investigated with the aid of a simple numerical model showing how and why they occur. The remainder of the chapter will then describe two examples of state-of-the-art diode laser pumped, cw-ICOPOs which are designed to obviate the problem of relaxation oscillations without losing any of the significant advantages which the intracavity technique confers.

2. The power characteristics of optical parametric oscillators

Much has been written on the principles underpinning the operation of OPOs and we shall avoid repetition here. For a theoretical and analytical thorough discussion of the physical processes underpinning these devices the reader should refer to (Ebrahimzadeh & Dunn 1998). In this section we shall describe the different operating regimes of both intra- and extra-cavity OPOs and examine those best suited to each geometry. Finally, we shall briefly discuss a strategy for operating the ICOPO under optimal efficiency conditions.

2.1 Power characteristics and the advantage of the intracavity technique

It is a common misconception that the ICOPO is somehow fundamentally superior to the ECOPO in terms of conversion efficiency, due to its much lower external threshold pump

power requirements. Whilst this is certainly true at lower powers, where the ICOPO is capable of efficient output when the ECOPO would not even be able to achieve threshold, at higher pump powers we shall see that the ECOPO is also capable of exhibiting excellent conversion efficiency. The crucial disadvantage of the ECOPO is its large offset threshold pumping power requirement.

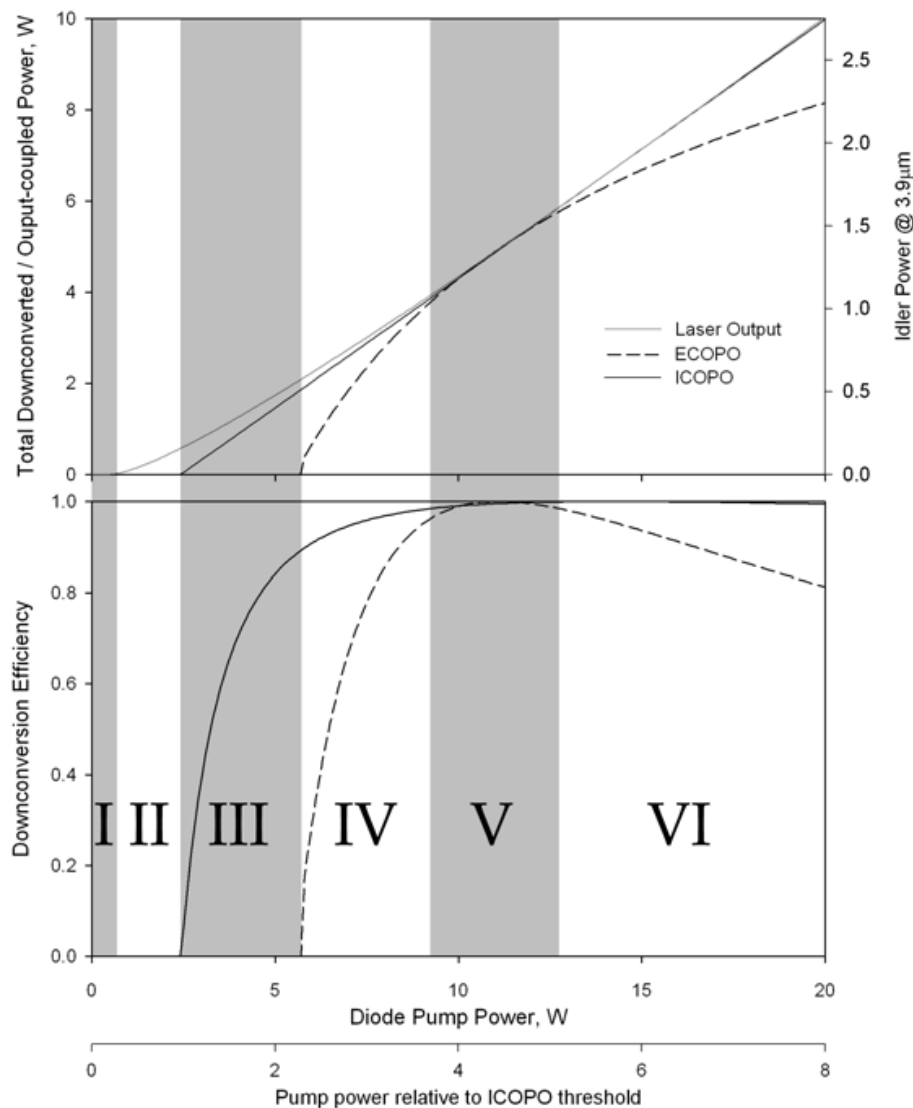


Fig. 4. Down-conversion characteristics of IC- and EC-OPOs

Even with high quality, modern nonlinear crystals exhibiting a high nonlinearity and interaction length, the finite cavity round trip loss for the down converted wave sets the minimum attainable ECOPO threshold in the region of $\sim 2\text{-}5\text{W}$, which would require at least $5\text{-}10\text{W}$ of primary optical diode pump power *simply to reach threshold*. However, once above threshold the down conversion efficiency (that is, the fraction of incident pump power down converted to longer wavelengths) rapidly increases to the point at which 100% down conversion efficiency is achieved once the ECOPO is pumped ~ 2.5 times above its threshold level (Ebrahimzadeh & Dunn 1998). A good example of this is (Bosenberg, Drobshoff et al. 1996) where $\sim 93\%$ of the incident $1\mu\text{m}$ pumping power was down converted into signal and idler power. ECOPOs have enjoyed something of a revival in recent years due to the

availability of high power, high spatial and longitudinal mode quality fibre lasers and the drop in cost of their associated diode laser pumping modules. The requirement to operate these devices 2-3 times threshold, and the limitations in nonlinear crystal interaction length / nonlinearity and finite signal round-trip loss, still results in the requirement for many 10's W electrical power required in order to operate these devices efficiently. Such a requirement precludes the realisation of the ECOPO in compact, low power designs.

The various operating regimes in which the devices can be operated are shown graphically in Fig. 4, where the output power characteristics of the parent pump laser, an ECOPO and an ICOPO are contrasted. In this model, a typical parent laser is assumed (i.e. Nd:YVO₄, pumped by an 808nm laser, ~2% round trip parasitic loss) and the linear loss effects of the intracavity OPO components is ignored. A note on nomenclature: "down-conversion efficiency" and "down-converted power" refer to the total power converted through the parametric process, i.e. both idler *and* signal. In general, only the longer wave idler is of interest and none of the signal is usefully extracted (although this need not be so - output coupling of the signal field is perfectly possible if this wavelength is also required). Therefore, a second axis has been added in the figure to indicate the total idler power obtained from the device, taking into account the quantum defect between the diode pump and generated idler field wavelengths.

So that the performance of each pumping geometry can be better compared, the threshold condition of the ICOPO and ECOPO in the model have been tailored such that maximum efficiency in either case occurs at the same pumping power (in this example, at about 11.5W). In reality this means artificially increasing the threshold of the ICOPO (by modelling the pump and signal field with only a very weak focus in the nonlinear material); real-world ICOPOs exhibit OPO threshold at far lower pumping powers than shown here - as little as a few hundred mW (Stothard, Ebrahimzadeh et al. 1998). We can see that Fig. 4 has been separated into 6 'zones' of operation. The first and second are merely below and above laser threshold, respectively. The ICOPO comes to threshold at the beginning of zone III, still well before threshold occurs in the ECOPO. In zone IV, ECOPO operation is achieved but the down converted power is still significantly less than in the case of the ICOPO. Clearly, if the available pump power were limited to the range ~2.5-8W then the ICOPO is obviously the superior choice in terms of the amount of mid-infrared light generated. As the down-conversion efficiencies in either case become optimised (i.e. near unity), the total down-converted power is comparable in each case (zone V) and there is little to differentiate between the two devices in terms of performance. In order to optimise for maximum overall efficiency, both devices would be operated in this zone. As the pump power is increased beyond the optimum operating condition (zone VI), the efficiency in each case drops (markedly so in the case of the ECOPO). Here, back conversion of the signal and idler takes place. In practice, one would not operate either device in this zone; in order to obtain very high output powers and maintain optimal efficiency the threshold of each OPO would be *increased* such that optimal down conversion (zone IV) occurs at the required operating point. The crucial advantage of the ICOPO over the ECOPO is that in a practical device, zone V can be achieved at very much lower primary pumping levels, whereby a combination of very high efficiency and moderate down-converted output power is possible. In the ECOPO, high efficiency is only achievable at ~2.5x threshold. As this threshold is locked at relatively high powers by the finite parametric gain / signal wave loss product (~2-5W of incident pumping power), high efficiency only occurs when very high powers are being obtained. For clarity, we summarise these operating regimes in tabular form.

Zone	Operating Regime	Notes
I	Laser below threshold	
II	Laser above threshold	
III	ICOPO above threshold	If diode pump power is limited then ICOPO performance clearly superior over these zones
IV	ECOPO above threshold	
V	Down conversion approaches 100%	Little to differentiate between devices in terms of down-conversion performance
VI	Over pumping	Would never operate either device here in practice

Table 1. Summary of the operating 'zones' depicted in Fig. 4

In the above treatment, the linear loss of the intracavity OPO components placed within the parent pump laser is ignored. In the case of the ECOPO, the pump is only used on a single pass and so linear loss effects, to a first approximation, have little impact upon performance. However, placing lossy components within a laser cavity has obvious consequences in terms of laser performance. With reference to Fig. 2(b) we see that the two additional components which the laser cavity must tolerate are the dichroic beamsplitter and nonlinear optical crystal. Clearly, these components must be antireflection coated in order to minimise loss at the pump wavelength. It is particularly important to secure the finest coatings available upon the nonlinear crystal and inner surface of the beamsplitter as these need to be specified at three separate wavelengths. However, coating techniques have now matured to the point at which such advanced coatings are generally obtainable, particularly in devices which do not require broad tuning of the OPO (and, hence, broad-band AR/HR coatings). For a well established nonlinear crystal such as PPKTP or PPLN, absorption at the pump wavelength is negligible and so the additional round trip loss of the ICOPO components can be as low as ~3-5% at the pumping wavelength. Significant crystal-induced loss is only encountered, and is therefore problematic, when the intracavity technique is used in conjunction with lossy nonlinear materials, such as ZGP pumped at $\sim 2\mu\text{m}$. In this case, care has to be taken that the round trip loss of the laser cavity accommodating such lossy components does not impact too heavily on the attainable circulating field and, hence, obviate the advantage that the intracavity technique confers. The use of such crystals is beyond the scope of this chapter.

2.2 ICOPO efficiency optimisation

Unlike the case of a laser, minimizing the point at which the ICOPO comes to threshold (in terms of the primary pump power from the laser-diode) does not necessarily bring about the highest output (or efficiency) at the maximum available pump power. This is because the nonlinear parametric process acts as the output coupler for the laser, and so for a given pumping power one requires that the OPO operates in such a way that it behaves as an optimal output coupler for the pump cavity (i.e. is operating in zone V (Fig. 4) for a given primary pumping power). Therefore, the threshold level of the OPO, in terms of external pumping power, is a function of both laser threshold and the external pumping power at which the device is to be optimised. If the OPO comes to threshold too quickly, then at the maximum available primary pumping power the laser will be over coupled, hence reducing the down-converted power obtained. For a particular value of laser threshold and maximum available primary pumping power, optimum down-conversion efficiency occurs when the condition

$$P_{th}^{OPO} = \sqrt{P_{th}^L \cdot P_{in}} \quad (1)$$

is met (Colville, Dunn et al. 1997), where P_{th}^L and P_{th}^{OPO} are the primary pump powers at which the laser and OPO, respectively, reach threshold, and P_{in} is the primary pumping power at which the device is to be optimised. When operated in this regime, the ICOPO acts as an optimum output coupler to the parent pump laser and maximum conversion of primary pump to down-converted power is achieved (this power being equal to that extractable from the pump laser under optimal output-coupling conditions with the OPO components accommodated within the pump cavity but with down-conversion suppressed).

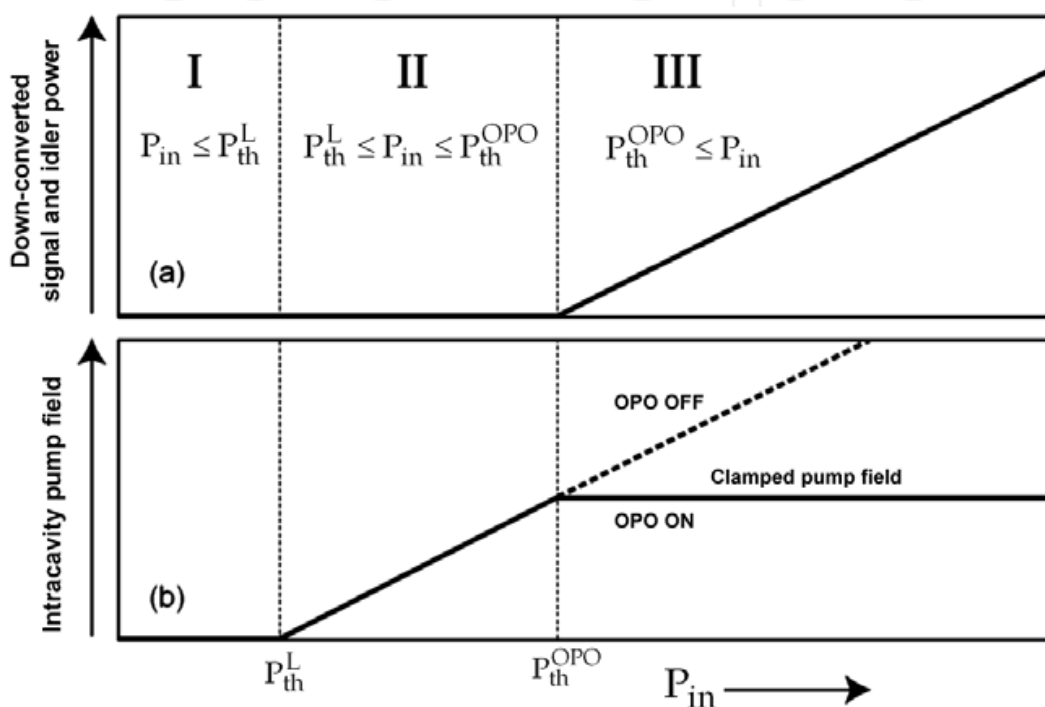


Fig. 5. (a) Linear output power of OPO once above threshold and (b) clamping effect of the ICOPO upon the circulating field (Turnbull, Dunn et al. 1998)

Whilst a very low value of P_{th}^{OPO} is highly desirable when the available primary pumping power is limited, reduced down-conversion powers are experienced when higher power pump sources are used as the system is operated too many times above threshold (because of the aforementioned over coupling of the pump field). Due to the high pumping fields available when using the intracavity technique, coupled with the low parametric thresholds enabled by long interaction-length, high-nonlinearity periodically-poled crystals, a choice can therefore be made when optimising the performance of the device either for maximum down-converted power or minimising parametric threshold in terms of primary pump power. Both of these cases are considered in a practical system later on in section 5.2.

Once above threshold, the parametric oscillator acts like an optical zener diode and 'clamps' the circulating field at the OPO threshold value, as shown in Fig. 5(b). Increased pumping power is then transferred from the laser gain medium population inversion, through the circulating field into increased power in the signal and idler waves, which grow linearly. When characterising the performance of an ICOPO, it is often well worth measuring the

quality of the pump-field clamping above OPO threshold as the primary diode pump power is increased. Good clamping is indicative of a well designed pump and signal cavity which is either free of (or robust in the presence of) any dynamic thermal effects which may be present within the laser gain medium and nonlinear optical crystals. Significant thermal lens effects manifest themselves in poor clamping of the pump field and a non-linear relationship between primary pumping and down-converted power. We shall see examples in the following section of how to calculate the circulating field required to bring the OPO to threshold, and experimental observations of the pump-field clamping effect.

Let us now take these simple design rules and see how they are applied when planning, constructing and characterising a system on the optical bench.

3. Designing a cw-ICOPO

In this section we shall take a specific example of a previously demonstrated ICOPO system reported in the literature (Stothard, Ebrahimzadeh et al. 1998) and walk through the process of realising such a device, ensuring that the first-time experimentalist will maximise his or her chances of success – by which we primarily mean at least getting the OPO above threshold. Here we will assume the experimenter has access to readily available pumping sources, Nd laser gain media and nonlinear crystals.

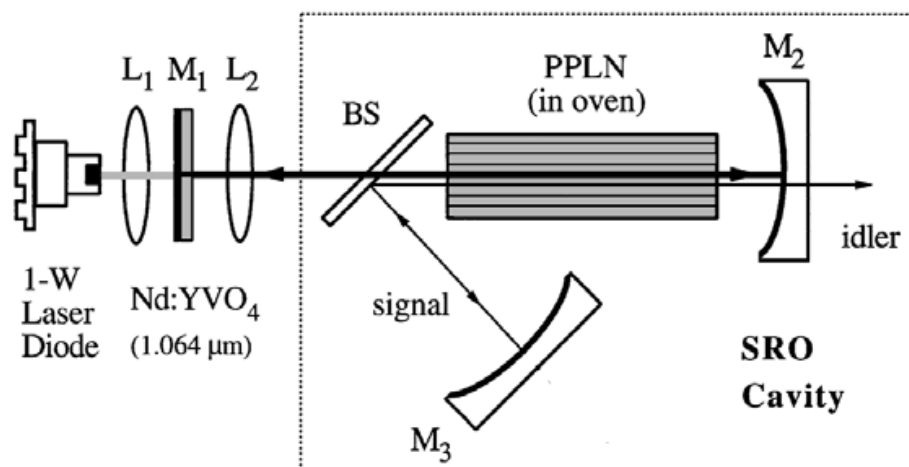


Fig. 6. A simple cw PPLN- Nd:YVO₄ ICOPO (Stothard, Ebrahimzadeh et al. 1998)

Our requirement is that the device, once constructed, will operate comfortably above threshold, delivering 10's mW of tunable power in the down-converted waves. Steps to circumvent the onset of relaxation oscillations will not be addressed in this discussion; here we will restrict ourselves to simply realising a low threshold, high efficiency device. In particular, we will consider the practical design choices which were taken in order to realise the first ICOPO based upon Nd as reported in (Stothard, Ebrahimzadeh et al. 1998), and use the physical parameters as used in that case. A schematic of that device is shown in Fig. 6.

The system was pumped by a c-packaged, temperature stabilised diode laser capable of delivering just 1W of optical power into the rear face of a 1% doped Nd:YVO₄ laser crystal. The laser cavity was defined by a highly reflective (at 1.064μm) coatings applied directly to the outer-most facet of the laser gain crystal and mirror M₂. All of the components within the cavity were anti-reflection coated, such that the round trip loss experienced by the pump field was ~3%. Mirror M₂ was also coated to be highly reflecting at the signal wavelength,

as was M3 and the dichroic beamsplitter BS, thus defining the signal cavity. Due to the limited diode pump power available (only 1W), a crystal exhibiting a high nonlinearity / length product (more on this in the following section) was required in order to minimise parametric threshold, and so a 50mm long PPLN crystal was procured. This was placed within an oven to avoid the effects of photorefractive damage.

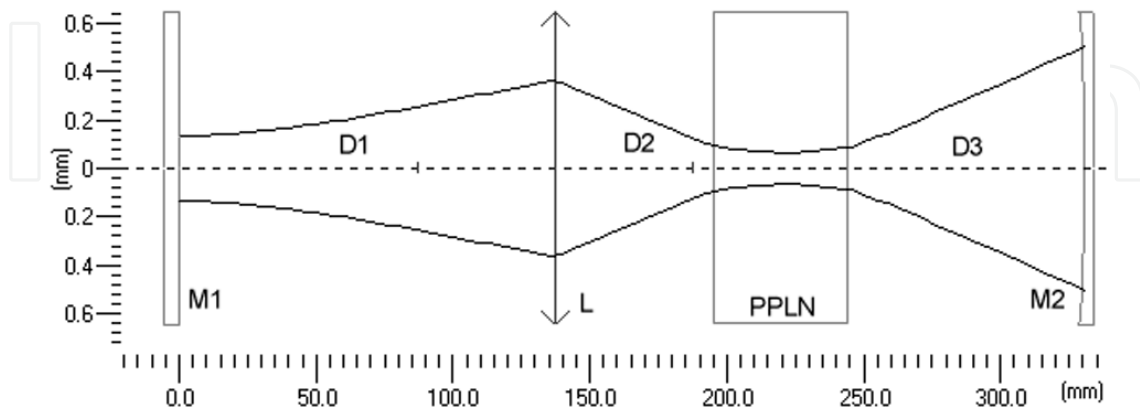


Fig. 7. Stability simulation of the pump cavity. Note that the beamsplitter has no focal power and is therefore omitted. Its optical length is incorporated into distance D2.

The cavity was modelled and its pump mode diameter, as a function of cavity position, is shown in Fig. 7. It is important that the cavity remain stable over a wide range ($\sim 50\text{mm} \rightarrow \infty$) of thermally-induced (by the diode pump) radius of curvatures modelled in mirror M1. Note the somewhat large distance D3 between the PPLN crystal and M2; this was set by the mirror substrate radius of curvature available at the time of the experiment (200mm). Such a long distance and the use of a relatively weak focal-length mirror results in a somewhat “loose” cavity, more susceptible to the effects of thermally-induced lensing prevalent in the PPLN crystal. A better solution is to use a substantially shorter curvature mirror, perhaps 25mm, placed close in to the PPLN crystal. This has the added advantage of increasing the free-spectral range of the pump cavity: helpful when trying to line-narrow the pump field.

3.1 Parametric gain and threshold

Clearly, it is of crucial importance that the OPO exhibits a threshold pumping requirement that is significantly less than the circulating pumping field available within the cavity of the pump laser, so ensuring that the threshold pumping level can comfortably be reached and exceeded. Let us examine the physical parameters which effect this level, and the steps which can be taken in order to minimise it.

When pumped by a polarized laser beam exhibiting sufficient spectral and spatial coherence, a nonlinear optical crystal designed for use in an OPO will exhibit fluorescence (i.e. gain) over its phase-matched bandwidth in much the same way that a laser crystal will exhibit gain over its gain-bandwidth (albeit by a different physical process). This gain is given by (Vodopyanov, 2003)

$$G = \frac{P_{\text{out}}}{P_{\text{in}}} - 1 = \sinh^2(\Gamma \ell) \quad (2)$$

where ℓ is the length of the nonlinear crystal and Γ is the gain increment given by

$$\Gamma^2 = \left(\frac{d_{\text{eff}}^2}{n^3} \right) \frac{2\omega_s \omega_i I_{\text{pump}}}{\epsilon_0 c^3} = \left(\frac{d_{\text{eff}}^2}{n^3} \right) \frac{8\pi^2 I_{\text{pump}}}{\lambda_s \lambda_i \epsilon_0 c} \quad (3)$$

Here, I_{pump} is the power density of the laser mode within the crystal, ω_s , ω_i , λ_s & λ_i represent the signal and idler angular frequency and wavelength, d_{eff} is the effective nonlinearity of the nonlinear crystal and n^3 is the product of the nonlinear material refractive index at the three transmitted wavelengths. Note that the factor d_{eff}^2/n^3 is referred to as the *figure of merit* (FOM) and indicates that a high nonlinearity alone does not necessarily yield high gain: it is moderated by ever-increasing refractive index. This is particularly important at longer signal and idler wavelengths where transparency issues mandate the use of semiconductor-based nonlinear crystals whose refractive indices are significantly larger than their phosphide- or arsenide-based counterparts. At low gains ($\Gamma \ell \leq 1$, as is experienced in the cw-regime), equation (2) approximates to

$$G_{\text{cw}} \approx \Gamma^2 \ell^2 \quad (4)$$

And therefore, when properly phase-matched, the single pass gain has a quadratic dependence upon $\Gamma \ell$. The full expression describing the parametric gain experienced as a function of circulating pump power P_{circ} , when the OPO is placed within the cavity of the pump laser, is then

$$G_{\text{cw}} = \left(\frac{d_{\text{eff}}^2}{n_p n_s n_i} \right) \frac{4\omega_s \omega_i \ell^2 P_{\text{circ}}}{\epsilon_0 c^3 \pi (\varphi_p^2 + \varphi_s^2)} \quad (5)$$

Where the refractive index at each of the propagating waves is now explicitly stated, as is the radii of the confocally-focussed pump and signal beams, φ_p and φ_s . This waist radius is given by

$$\varphi_\lambda = \sqrt{\frac{\lambda \cdot \ell}{2\pi}} \quad (6)$$

Note the factor of 2 increase in (5) over (2); this is a consequence of the signal field experiencing gain on each pass of the pumping field, which is of course travelling in both directions through the nonlinear crystal on each round-trip of the pump cavity. Threshold occurs when the circulating pumping field is sufficiently powerful that the parametric gain exceeds the round-trip loss experienced by the resonated down-converted (in this case, the signal) wave:

$$G_{\text{cw}} \geq \alpha_{\text{cav}} \quad (7)$$

Where α_{cav} is the round-trip loss of the signal cavity. Finally, therefore, we define P_{th} as circulating pumping field (*not* the threshold diode pump power) at which the OPO comes to threshold and re-arrange (5) to give

$$P_{\text{th}} = \frac{n_p n_s n_i \epsilon_0 c^3 \pi (\varphi_p^2 + \varphi_s^2)}{4\omega_s \omega_i \ell^2 d_{\text{eff}}^2} \cdot \alpha_{\text{cav}} \quad (8)$$

This relation, then, lets us examine the various parameters we can influence in order to attain parametric threshold for the minimum of circulating pump field and, hence, primary pump power. It also reminds us that we are always limited by the material properties of the crystals available to us and the wavelengths over which we wish the device to operate, and illustrates why advances in this field often go hand-in-hand with the development and improvement of new nonlinear materials.

Clearly, in order to obtain the lowest possible threshold we need to maximise the denominator of (8) which means utilising a nonlinear material which offers the largest $d_{\text{eff}} - \ell$ product. This is why, given the very modest primary pump power used in this experiment, the nonlinear material PPLN was selected: this crystal exhibiting a then unprecedented 17pm/V nonlinearity and available in lengths as long as 50mm. It is also clearly crucial to minimise the signal cavity round trip loss α_{cav} . When procuring the optical coatings applied to the beamsplitter and signal cavity mirrors it is wise to place most emphasis on the best specification at the signal wavelength. The coating applied to the inner face of the beamsplitter, which must be anti-reflecting at the pump wavelength and broad-band highly reflecting at the signal, is particularly challenging for coating manufacturers. When specifying this coating, it is often helpful to encourage the coating engineer to let the incidence angle and polarisation of the pump and signal waves 'float' in his or her modelling calculations (if these parameters are not fixed by other demands placed on the system design), thereby giving him or her the freedom to maximise the performance of this challenging coating. Typically, one can conservatively expect the round-trip loss of the signal cavity to be ~2-5% (i.e. $\alpha_{\text{cav}} \approx 0.02 - 0.05$).

The chosen length of the crystal, along with the desired signal and idler wavelengths, fixes the confocal beam waist radius of the two resonant beams, as given by (6). The refractive index of PPLN at the three different wavelengths is calculated using Sellmeier equations (which shall be addressed in the following section). For the particular case under discussion, where the pump, signal and idler wavelengths were ~1.0, 1.5 and 3.6 μm respectively, and a signal cavity round trip loss estimated to be 4%, we find upon solving (8) that parametric threshold occurs when ~3.5W is circulating within the pump cavity.

We now need to assess whether this intracavity field can be comfortably reached and exceeded with the available pumping power. With knowledge of the gain parameters of the laser gain medium and cavity (upper-state life time, stimulated cross-section, pump mode intensity, parasitic loss, etc.) the relation between the primary diode pumping power and the circulating pump field can be accurately modelled. However, it is often more straight forward to simply measure the output power of the laser through a well-chosen output coupler and then infer the intracavity field. For instance, with mirror M2 in Fig. 6 removed and replaced with an (optimal) 5% transmissive output coupler, 510mW of power at the pump wavelength was extracted. This indicates that 10W of field was circulating within the cavity, easily enough to bring the OPO to threshold when the laser is tolerating the additional loss of the output coupler. When highly reflecting mirror M2 was replaced, we estimated that the circulating field increased above 20W – enough to place the OPO well above threshold.

In marginal threshold cases it is possible to lower the threshold requirements of the OPO by increasing the intensity of the resonant fields within the nonlinear crystal. This is achieved by reducing the spot sizes of the pump and signal waists φ_p and φ_s . This however results in less optimised operation at higher pumping powers and can have practical consequences

such as mode aperturing at the facets of the crystal, increased susceptibility to the effects of thermal lensing (and, in extreme cases, optical damage) but is a useful trick to try when out of other options.

3.2 Phase-matching and tuning

Much has been written about phase matching in nonlinear optical processes and for the sake of space it will not be repeated here save for a brief overview. Most applications to which the ICOPO will be turned will require the production of a specific idler and, hence, signal wavelength pair. Many applications (e.g. spectroscopy) also place both a coarse and fine tunability requirement on the device. For energy conservation, the signal and idler wavelengths are related to that of the pump by the relation

$$v_p = v_s + v_i \quad (9)$$

or, more usefully,

$$\frac{1}{\lambda_p} = \frac{1}{\lambda_s} + \frac{1}{\lambda_i} \quad (10)$$

This, however, implies an infinite combination of signal and idler wavelengths for a given pumping wavelength. How does one successfully achieve device operation at the required signal and idler wavelengths?

The particular signal and idler frequency pair that is generated is governed by the *phase-matching* criterion of the nonlinear optical crystal employed. The efficient flow of power from the pumping wave into signal and idler waves only occurs when the three waves (pump, signal and idler) are travelling at the same speed (i.e. are in phase) within the nonlinear medium. When this condition is satisfied then the process is said to be phase-matched. Clearly, this criterion cannot be met in isotropic media due to linear refractive dispersion and so more subtle phase-matching schemes are called for. Phase-matching has traditionally been achieved by using bi-refrident crystals through which the waves were propagated at an appropriate angle and polarisation with respect to the crystallographic axis such that the respective refractive indices experienced by the different wavelengths were equal, satisfying the condition

$$\frac{n}{\lambda_p} - \frac{n}{\lambda_s} - \frac{n}{\lambda_i} = 0 \quad (11)$$

Unfortunately these angles of propagation rarely coincided with that which the optimal nonlinearity of the material was encountered, leading to low overall nonlinear coefficients. In addition, tuning of the signal and idler waves was often achieved through rotation of the crystal angle, thus leading to complicated mechanical designs required to keep the optical cavity stable whilst crystal rotation took place. This changed with the advent of periodically poled nonlinear media where the phase-matching criteria could be “engineered” into the material by periodic inversion of the crystallographic domains (as shown in Fig. 8(a)), thereby making the generated signal and idler wavelengths simply a function of polling period (and crystal temperature). This enabled the somewhat cumbersome tuning mechanisms associated with conventional bi-refrident phase-matched devices to be dispensed with. The axis of propagation could also now be chosen in order to access the

highest material nonlinearity. We shall only concern ourselves with these *quasi-phase-matching* (QPM) schemes in this discussion as all of the devices described in this chapter utilised this method of phase matching

The period Λ of the domains (often called the *grating period*, but not to be confused with diffraction gratings) written within the nonlinear crystal is chosen such that it takes up the 'slack' in the phase-mismatch so that phase-matching is achieved:

$$\frac{n_p(\lambda_p, t)}{\lambda_p} - \frac{n_s(\lambda_s, t)}{\lambda_s} - \frac{n_i(\lambda_i, t)}{\lambda_i} - \frac{1}{\Lambda(t)} = 0 \quad (12)$$

Note that the refractive index of the material is a function of both wavelength and temperature. Due to thermal expansion of the nonlinear crystal as its temperature is varied, the grating period is also somewhat dependent upon temperature. It is the dependence of these parameters on wavelength and temperature, along with the need for the conservation of energy, which enables the OPO to be tuned by crystal temperature as well as and pump wavelength. Recently more advanced grating patterns have been demonstrated where the grating period varies linearly across the lateral axis of the crystal. In this, the so-called fanned grating design (Fig. 8(b)), the phase-matching condition is therefore a function of crystal position and very rapid tuning of the signal and idler can be achieved by translating the crystal through the circulating pumping field.

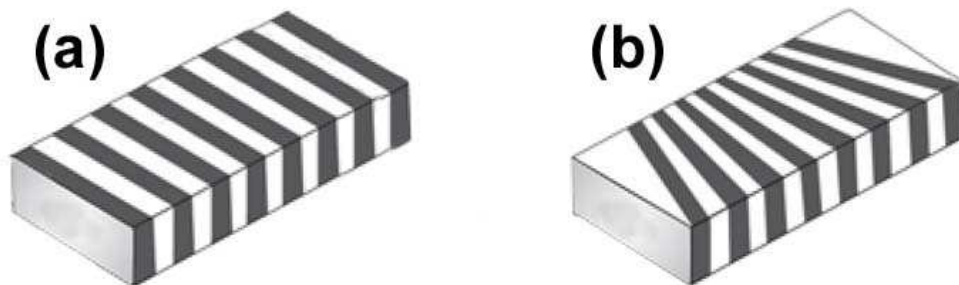


Fig. 8. Periodically-poled nonlinear crystals with (a) single and (b) fanned grating designs.

Relation (12) is solved by using empirically-derived Sellmeier equations which relate the refractive index of a particular material to the wavelength of light propagating within it. Modified Sellmeier equations also include temperature-dependence terms in order to enable the modelling of temperature tuning of the phase-matched condition. Not only is the format of each Sellmeier equation (and the constants used) specific to a particular nonlinear material, it is also often specific to the method of crystal growth used during manufacture. Whilst most commonly used nonlinear materials are very well characterised and their Sellmeier equations are available in the literature, it is often prudent to contact the crystal manufacturer and either ask which Sellmeier equations best describes their material, or better still let them calculate the required grating period in order to phase-match for the desired signal and idler wavelength pair at the required temperature.

The Sellmeier equation and its coefficients describing the PPLN nonlinear crystal used in this particular experiment is described in (Jundt 1997) and the accuracy with which it was able to predict the refractive index of the PPLN crystal and, hence, the phase-matched signal and idler wavelength pair for a given material temperature and grating period is shown in Fig. 9. The PPLN crystal used in the experiment had eight discrete grating zones of different

polling periods written within it and so Fig. 9 comprises eight pairs of signal and idler curves, each particular pair corresponding to a different grating zone.

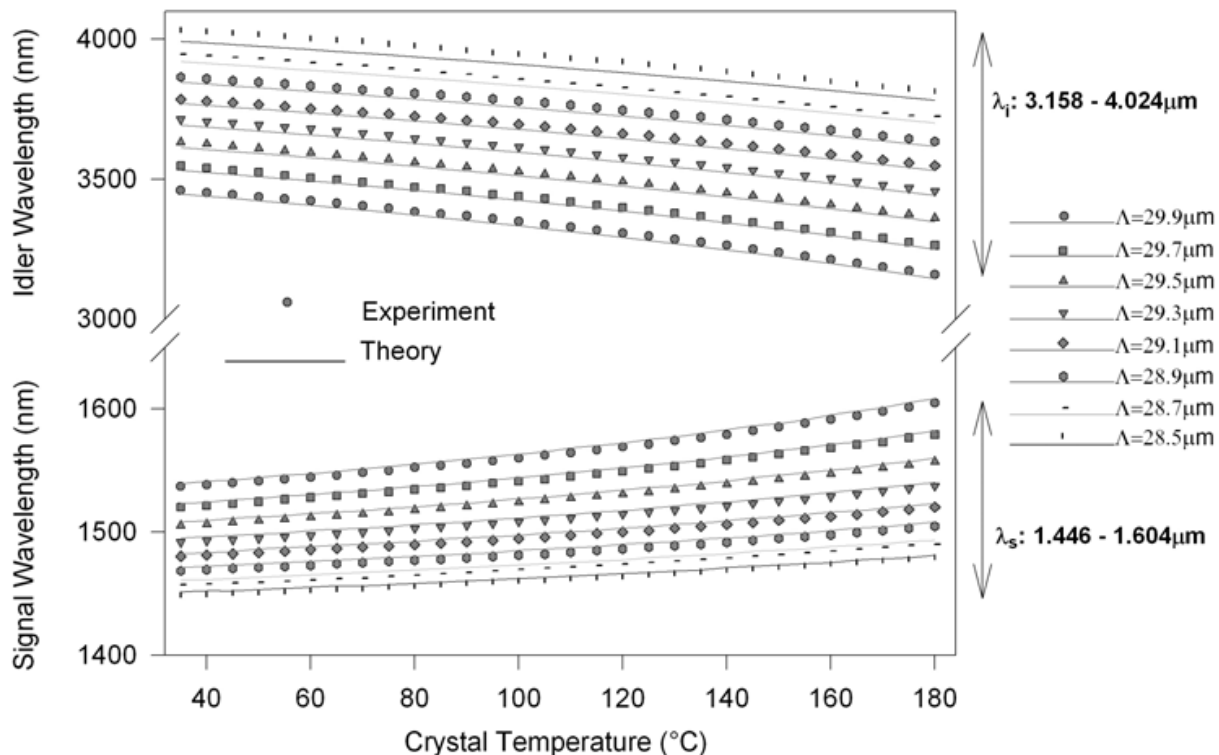


Fig. 9. Predicted and measured tuning of the signal and idler wavelengths

An accurate determination of the anticipated signal and idler wavelengths and tuning ranges is important, not only from the point of view of the end application of the device, as this information must be first determined before specifying the centre-point and bandwidth of the coating pertaining to the idler and, of particular importance for the reasons outlined above, the signal wavelength. The threshold pumping power requirement often rises substantially at the extremes of the tuning range as signal cavity round trip loss creeps in at the edge of the coating bandwidth. On condition that it does not compromise overall performance, it is often prudent to specify a coating bandwidth exceeding the tuning range over which the parametric process is expected to phase-match in order to obviate this effect.

3.3 Performance evaluation and optimisation

The down-conversion performance of the device is indicated in figure Fig. 10, where the extracted idler is shown as a function of increased primary diode pump power as is the circulating pump field both in the presence and absence of down-conversion. The laser and OPO threshold occurred at a diode pump power of 69 and 310mW respectively. In this latter case, 5.2W of circulating pump power was present, a figure somewhat larger than the anticipated threshold field of 3.5W. This is accounted for by sub-confocal focussing of the pump and signal fields resulting in reduced field intensity. Whilst this leads to the increase in threshold pump power, the cavity resistance to thermal lensing effects within the PPLN crystal was significantly reduced leading to more robust performance of the device. Despite this increase, the primary advantage of the ICOPO approach is still clear. In order to bring

the OPO to threshold in an extra-cavity system, 5.2W of power from the pumping laser would be required, which itself would therefore require ~ 10 W of primary optical pumping power. We achieve the same here for just 310mW of primary pump power – a significant drop indeed. The robust nature of the system is evident from the both linear relationship between the circulating field and pump power in the absence of parametric down conversion and the excellent clamping of the pump field once the OPO is above threshold. It is worth comparing the measured performance of the device as indicated in Fig. 10 with the theoretical behaviour shown in Fig. 5.

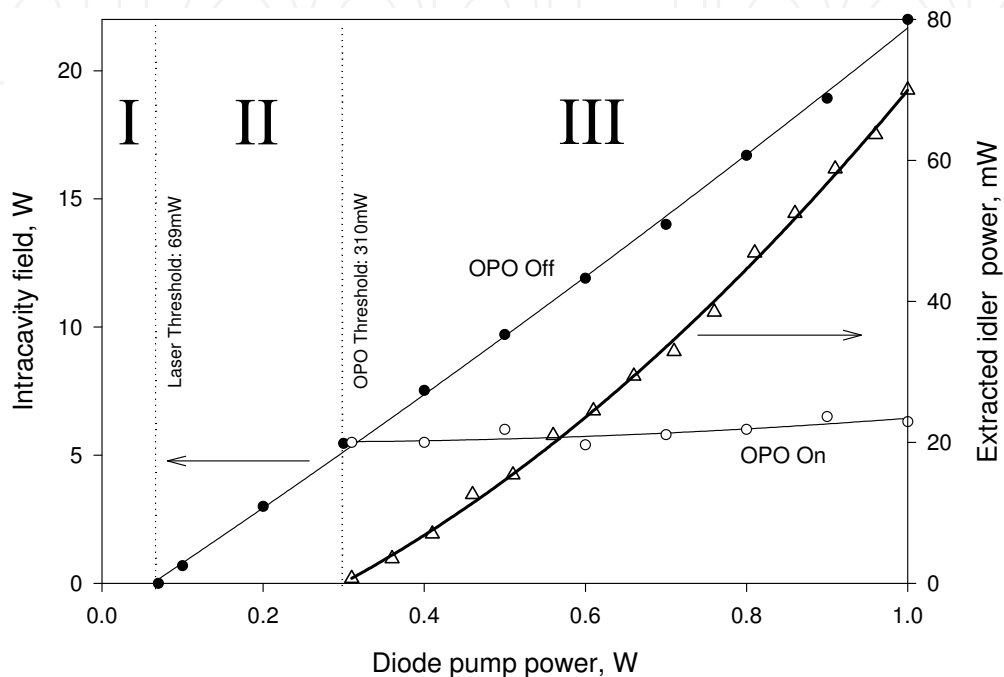


Fig. 10. Extracted idler (triangles) and pump-field with (open circles) and without (closed circles) operation of the OPO as primary diode pump power is varied. The idler wavelength was $3.66\mu\text{m}$.

The slightly super-linear nature of the extracted power is a consequence of a thermally-induced increase in the focal power induced in the Nd crystal reducing the mode size (and hence, increasing intensity) of the pump field within the PPLN crystal at higher primary pump powers

At the maximum pump power of 1W the device delivered 70mW of tunable idler through M2. In order to calculate the total down-converted power (that is, the total signal and idler power generated) we need to take into account the quantum defect between the signal and idler waves and for the fact that the idler is generated in both directions within the PPLN crystal (the 'other' direction being lost within the system). The total down-converted power is therefore

$$P_{\text{DC}} = 2 \cdot P_i \cdot \left(1 + \frac{\lambda_i}{\lambda_s} \right) \quad (13)$$

This, for an idler power of 70mW and an idler wavelength of $3.6\mu\text{m}$, corresponds to a total down-converted power of 476mW from the pump wave into the signal and idler. Recall that

when mirror M2 was replaced with an optimal output coupler for the pump cavity, 510mW of power at the pump was obtained. We can therefore take the *down-conversion efficiency* of the device (that is, the fraction of the total obtainable power which is down-converted) to be $476/510 = 93\%$. A down-conversion efficiency of unity can only be achieved when the OPO is optimally output coupling the pump field through the parametric effect, which is achieved when relation (1) is satisfied. For a laser threshold and operating pump power of 69 and 1000mW respectively, the optimal OPO threshold is then 250mW – slightly less than is the case in this system. As we have said, the stability of the cavity has been improved by slightly defocusing the pump (and signal) waists within the PPLN crystal which has raised the OPO threshold to this non-optimal level. The resulting improvement in performance, however, makes this slight drop in overall efficiency a price worth paying.

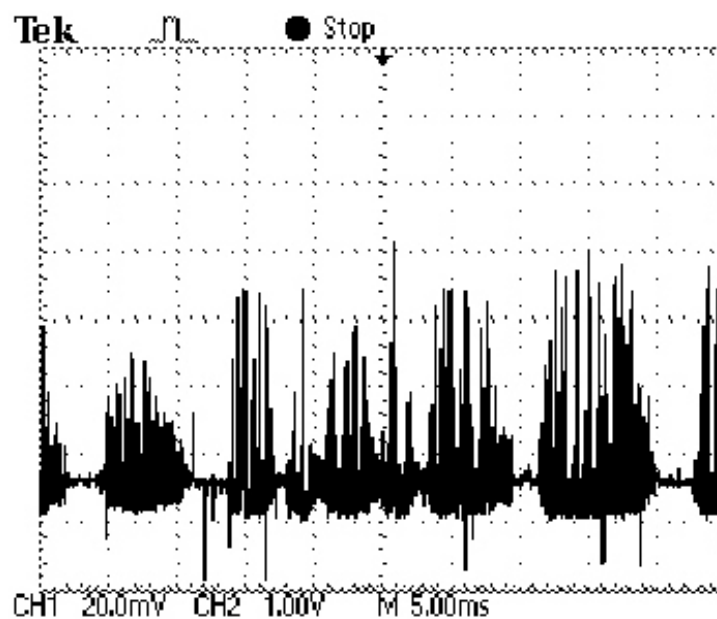


Fig. 11. Spontaneous and long-lived bursts of relaxation-oscillations manifesting themselves on the circulating pump field.

Finally, we turn our attention to the transient stability of the device which was measured by directing the small amount of pumping field reflected off of the rear face of the beamsplitter onto a fast photodetector. An example of the resulting trace is shown in Fig. 11. In the absence of any external perturbation mechanism the pump (and hence signal and idler) fields exhibited spontaneous and very long-lived bursts of high frequency relaxation oscillations. This resulted in $\sim 100\%$ modulation of the extracted idler field and erratic longitudinal mode hopping of the pump field, both of which are most undesirable in the context of high resolution spectroscopy and renders the device unsuitable for all but mean power, “crude” mid-IR applications. This is regrettable as in all other respects this system displays the very many highly desirable characteristics as discussed in sections 1 & 2,, such as very high efficiency, broad tunability, compact geometry, etc. In order to release the potential of this technology, a solution to the problem of relaxation oscillations is crucial. Let us now focus on the nature of these oscillations, the physical processes underpinning their behaviour and some real-life strategies for their elimination.

4. Transient dynamics and the origin of relaxation-oscillations

Whilst laser systems based upon Nd-doped gain media readily exhibit relaxation oscillations when substantially perturbed from their steady-state they do not, on the whole, display any stability problems when left to their own devices. Why is it, then, that a perfectly stable and well-behaved Nd laser should suddenly become prone to spontaneous burst of erratic and long-lived relaxation-like oscillations when an OPO is placed within its cavity?

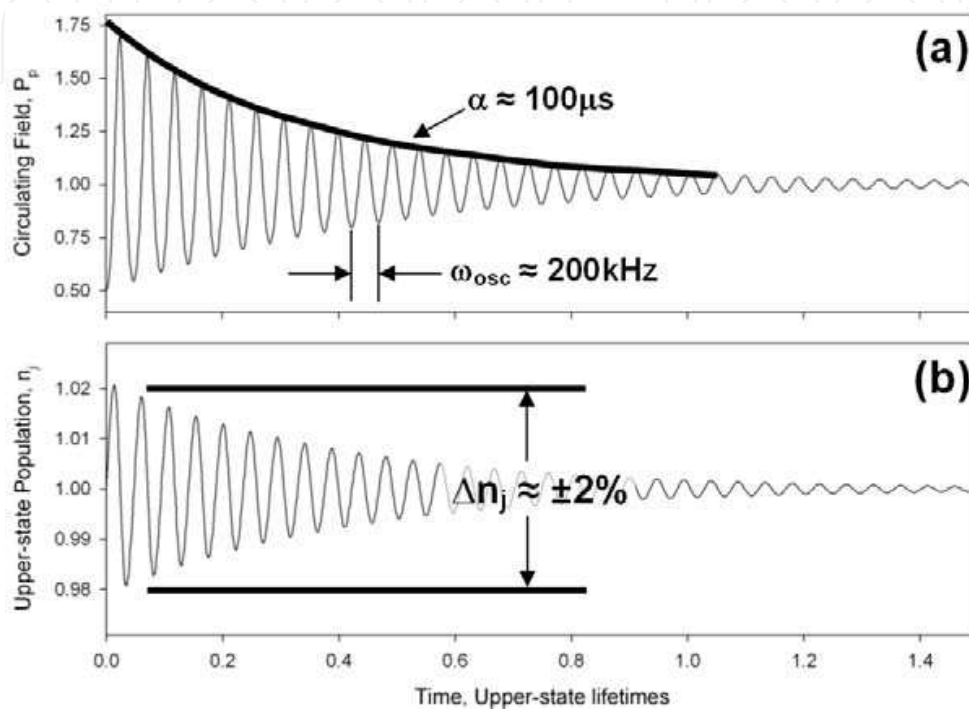


Fig. 12. Modelled relaxation-oscillation oscillations for a simple Nd-based laser. Photon (a) and upper-state (b) population evolution over time after the steady state is perturbed.

Experimental observation indicates that the relaxation oscillations displayed by ICOPOs are different in three key ways to those displayed by the parent pumping laser. They (a) are very long lived, (b) have a far higher oscillation frequency and (c) occur spontaneously. In this section we will explore the origins and the nature of relaxation oscillations in cw-ICOPOs, and thereby find potential strategies for their elimination.

Relaxation oscillations in laser systems are caused by interplay between the energy stored in the upper state of the lasing transition within the gain medium (n_j) and that stored within the optical cavity of the laser due to the circulating pump field (P_p). In the ICOPO, a third parameter, the energy stored within the signal cavity due to the circulating signal field (P_s) is also introduced. As all of these parameters are cross-coupled, it is useful to investigate their behaviour by constructing a set of coupled rate equations which can then be solved numerically with different starting parameters. In the case of the ICOPO, the three coupled rate equations might be as follows:

$$n_j' = \frac{1}{\tau_u} \cdot [1 + k - n_j - (k \cdot P_p \cdot n_j)] \quad (14)$$

$$P_p' = \frac{P_p}{\tau_p} \cdot \left[\frac{n_j \cdot \sigma_j}{1+k} - 1 - \frac{(\sigma_j - 1 - k) \cdot P_s}{1+k} \right] \quad (15)$$

$$P_s' = \frac{P_s}{\tau_u} \cdot [P_p - 1] \quad (16)$$

We say “might” as there is some freedom in the construction of these equations; it is up to the investigator to choose the way in which the model is normalised. In this particular set of expressions, n_j , P_p and P_s are assumed to be unity in the steady-state. The cavity photon lifetimes of the pump and signal cavities are given by τ_p , τ_s and the upper-state lifetime by τ_u . These parameters are normalized to the laser gain medium upper-state lifetime and so τ_u is always unity. The factors k and σ_j refer to the pumping levels of the laser and OPO with respect to their threshold conditions: σ_j is simply the number of times above threshold at which the laser is operated, and $(k+1)$ is equal to the number of times at which the OPO is operated above its threshold level.

Let us initially consider the dynamics of the laser operating in the absence of down-conversion. In practice this could easily be achieved by blocking the signal cavity without effecting the operation of the laser. Once running, the laser steady state is ‘plucked’ by instantaneously halving the circulating field. The numerical model is then allowed to run until the laser returns to the steady state. The results of this simulation are shown in Fig. 12. In this model the pump cavity photon lifetime was assumed to be 20ns and the upper-state lifetime 100 μ s (i.e. $\tau_u=1$; $\tau_p=0.0002$). We can see from the figure that once perturbed, the laser returns to its steady-state in about 100 μ s (i.e. about an upper-state lifetime), and has an oscillation frequency of about 200kHz. This frequency is determined by the mean of the upper-state and pump cavity photon lifetimes as:

$$\omega_{osc} \propto \sqrt{\frac{1}{\tau_u \cdot \tau_p}} \quad (17)$$

Thus we see that the very long upper-state lifetime (compared to that of the pump cavity photon) moderates the oscillation frequency to the relatively low ~100’s kHz range. This is crucial as this relatively low oscillation frequency gives the upper-state population time to “respond” to the variations in the circulating field. Upon close inspection of Fig. 12, it is clear that the circulating field and upper-state population are in quadrature-phase. It is a combination of this phase difference, and, crucially, the modulation depth of the upper-state population which is the primary damping mechanism returning the system to its steady-state after a perturbation event. In the case of the system modelled above, the $\sim \pm 2\%$ modulation depth of n_j is sufficient to return the system to its steady-state in about an upper state lifetime.

We now re-run the model using the same laser parameters, but this time in the presence of intracavity parametric down conversion. Here the system is simulated operating at 2 times OPO threshold ($k=1$) with a signal cavity photon lifetime of 40ns (i.e. $\tau_s=0.0004$). Fig. 13 shows the transient dynamics of the system after perturbation.

It is obvious that the inclusion of parametric down-conversion within the cavity of the laser has had an enormous impact upon the transient dynamic behaviour of the system. Even after 20 upper-state lifetimes has passed (i.e. 2ms) the oscillations have still yet to damp away.

Clearly, any system exhibiting such oscillations having triggering mechanism on the order of or less than this time would display semi-continuous oscillatory behaviour. The time scale used in Fig. 13 is such that the individual oscillations are not resolvable. These can be seen by re-plotting the figure over just a few fractions of an upper-state lifetime, as shown in Fig. 14 (a). We see now that as well as a sharp decline in the damping of the oscillations (giving rise to the very long oscillation events depicted in Fig. 13), the inclusion of the OPO within the parent pump laser has led to a very substantial increase in the oscillation frequency.

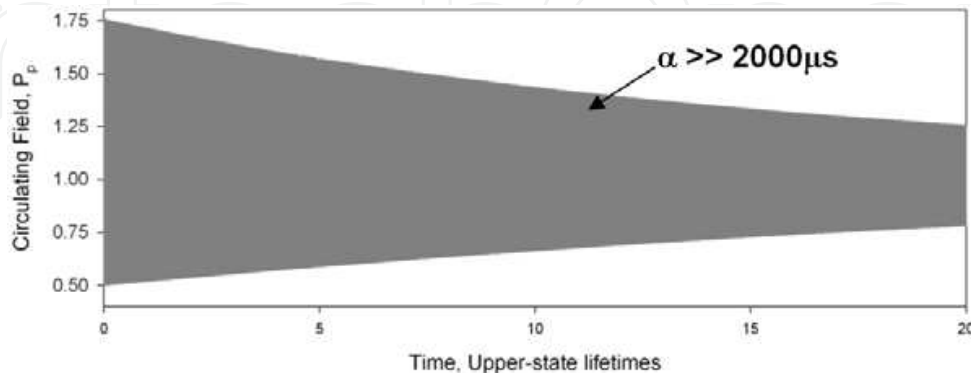


Fig. 13. Modelled relaxation-oscillation oscillations for a perturbed Nd laser based ICOPO. Note that the individual oscillations are not visible on this time scale.

We previously stated that in the case of the laser operating in the absence of the OPO the oscillation frequency was given by the upper-state and pump cavity photon lifetime (17). Now that the OPO is included in the system the processes giving rise to oscillations have shifted down a tier from upper-state population \rightarrow pump cavity power \rightarrow signal cavity power, and therefore the oscillation frequency is now independent of the upper-state lifetime. It is now solely governed by the pump- and signal- wave cavity photon lifetimes:

$$\omega_{\text{osc}} \propto \sqrt{\frac{1}{\tau_p \cdot \tau_s}} \quad (18)$$

The relatively long lifetime of the upper-state, compared to that of the pump- and signal-cavity photon lifetimes, is now no longer able to moderate the oscillation frequency and the very short lifetimes of τ_p and τ_s result in such high, order-of-magnitude increased oscillation frequencies.

Whilst the influence of the upper-state lifetime upon the oscillation frequency has been removed in the ICOPO, its population response to the changing circulating pump field is still the primary damping mechanism for the system. This is problematic as the very high oscillation frequencies have a serious impact upon the ability of the upper-state population to respond to the rapidly changing circulating field. This is somewhat analogous to the charge on a large capacitor being unable to track a high-frequency signal placed across its plates.

The resulting upper-state population is shown in Fig. 14(b). The modulation depth has now been sharply reduced by two orders of magnitude to just $\pm 0.02\%$, i.e. just 1 part in 10^4 . This explains why the oscillations, once induced, carry on for so long – there is very little damping within the system. It also shows why the oscillations are so easily triggered as only

very small excursions in the upper-state population are necessary to begin an oscillation event. Such an excursion could be caused by an acousto-mechanically induced longitudinal mode-hop of the circulating pump field or small modulation in the primary pumping field. The long upper-state lifetime (compared to the oscillation period) precludes the use of a feedback system between the circulating pumping field and external primary pump power modulation as a mechanism to improve the damping in the system as it acts as an “optical capacitor”; even 100% modulation of the primary pumping diode scarcely effects the upper-state population on the time scale of the oscillation periods indicated in Fig. 14.

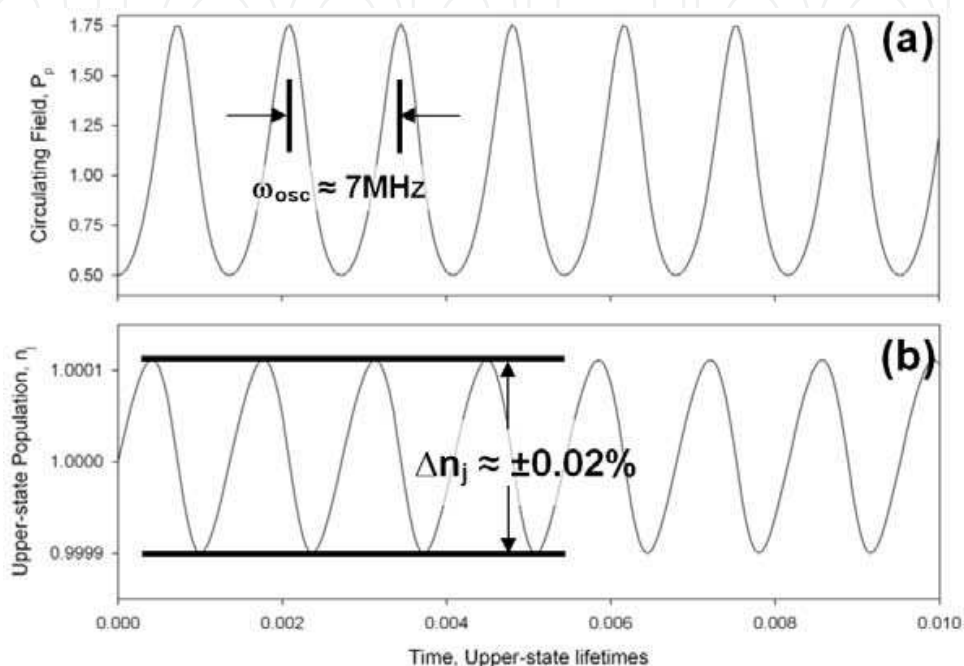


Fig. 14. Modelled results as in Fig. 13 but also showing the upper-state population and with a much enlarged time axis.

To summarise: we have shown, through the use of a simple numerical model based upon a set of three coupled rate-equations, that it is (a) the high oscillation frequencies associated with ICOPOs, brought about by high-speed energy transfer between the pump and signal wave cavities via the parametric process, coupled with (b) the weak damping induced onto these high frequency oscillations by the very long upper-state lifetime of the laser gain medium which leads to both high susceptibility to, and such long bursts of, relaxation oscillations in Nd-ICOPOs. In the next section, we examine ways in which the problem of relaxation oscillations can be circumvented by examining two state-of-the-art cw-ICOPOs which both display excellent transient stability.

5. Examples of practical, relaxation-oscillation free cw-ICOPOs

In the previous sections we have touched upon the various parameters governing the operation of cw-ICOPOs and looked in some detail at the physical processes underpinning the poor transient dynamic behaviour of these devices. We now turn our attention to two practical examples of state-of-the-art diode-pumped cw-ICOPOs which have been engineered with particular emphasis on the elimination of the relaxation oscillations which have to date severely restricted this technology from reaching its full potential.

5.1 Relaxation-oscillation suppression through second-harmonic generation

We have seen that a combination of the long upper-state lifetime of Nd-doped laser gain materials coupled with the high-frequency oscillations resulting from rapid power flow from the pump, through the parametric process, to the signal cavity leads to very weak damping and, hence, long oscillation times. One potential route to break this cycle is the inclusion of an additional damping mechanism within the system. Such a scheme could be introduced actively by utilising a fast detector to monitor the circulating pump or signal field strength, and then somehow instantaneously feed this back onto the loss of the respective cavity. Fig. 15 shows such a technique implemented in the schematic ICOPO depicted in Fig. 2(b).

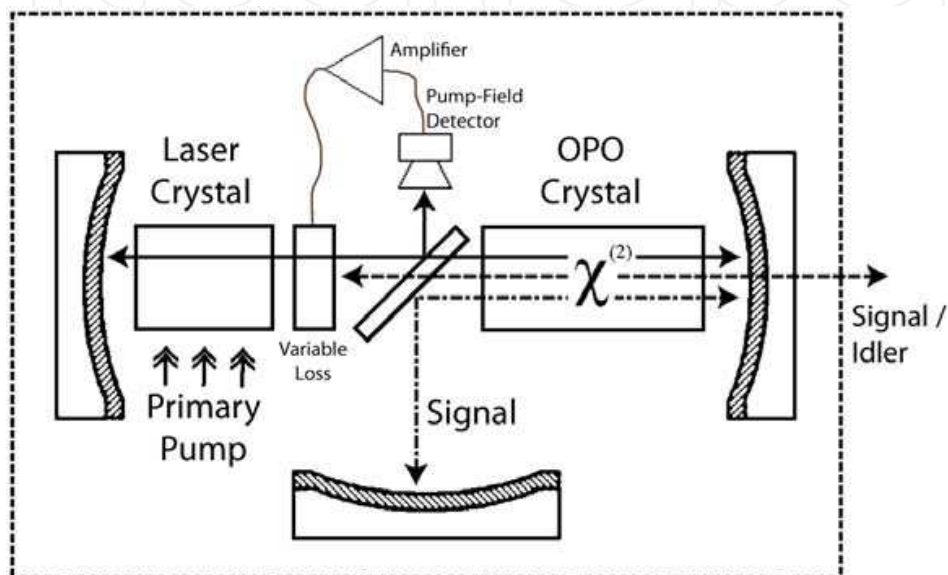


Fig. 15. Potential active scheme to eliminate relaxation-oscillations via an active damping mechanism

In this device, the small amount of circulating pump field which reflects off of the (anti-reflection coated) beamsplitter is directed towards the fast photodetector. The signal from this detector is then amplified and buffered before being fed into a loss mechanism; perhaps an acousto- or electro-optic modulator. This loss mechanism modulates the loss of the pump cavity and, hence, the cavity photon lifetime thus forming a negative feedback loop which preferentially suppresses the high intensity peaks of the oscillations and significantly reduces their damping time. Numerical modelling of this technique indicates that the dynamics of the system are modified to the point at which the oscillation decay time is potentially even shorter than those exhibited by the laser in the absence of the parametric process. In practice, though, the finite bandwidth of the feedback loop described here would introduce an unacceptable phase lag between the peaks of the oscillations and the modulation of the intracavity loss, a problem exacerbated by the high frequency of the oscillations and their higher-harmonic spectral components ($>10\text{MHz}$), the requirement for very fast electronic amplification and, in the case of an acousto-optic modulator, the acoustic wave front time-of-flight between the transducer and the pump field beam within the modulator medium.

A very attractive alternative scheme based upon this philosophy (i.e. pump-cavity photon lifetime dependence upon pump-field intensity) is facilitated by placing a nonlinear

frequency-doubling (or second-harmonic generation (SHG)) crystal within the pump-wave only section of the pumping cavity, as shown in Fig. 16. Such a scheme is a successful oscillation damping mechanism as the second-harmonic conversion efficiency (and hence its 'loss' within the pump cavity) is proportional to the *square* of the power propagating within it. The higher intensity peaks of the oscillations are therefore preferentially attenuated compared to the troughs. This scheme has many highly desirable characteristics in the context of relaxation-oscillation suppression, most notably that the process of up-conversion is instantaneous (i.e. there is no phase lag between the increase in pump intensity and the corresponding drop in pump cavity photon lifetime) and, particularly attractive in the context of practical devices, is entirely passive.

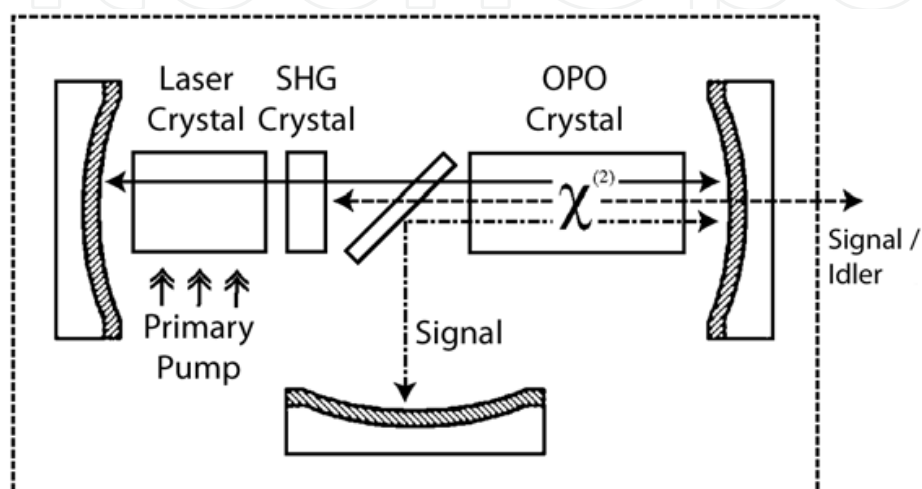


Fig. 16. CW ICPO with SHG relaxation-oscillation suppression.

In order for this scheme to operate correctly, it is important that a small amount of the circulating pumping field is lost to up-conversion even in the steady state. Clearly, as SHG has no threshold associated with it (unlike the parametric down-conversion), some frequency doubling will always be present as long as the pump laser is above threshold. This "bias" loss level, and indeed the amount of SHG which occurs in the presence of relaxation oscillations, can be controlled by variations in (a) the length of the SHG crystal, (b) the choice of focussing of the circulating pump field within the SHG crystal, (c) the choice of SHG crystal and (d) variation in the up-conversion phase-matching condition. In practice it is variations in this latter parameter which is most straight forward to implement as it can be varied in real time (in the case of temperature tuning of the phase-matched condition) without otherwise impacting upon the operation of the pumping laser. The clamping effect of the OPO upon the circulating field results in comparatively low levels of green light generation, as the field will typically be held at $\sim 2\text{-}4\text{W}$ by the OPO. When the scheme is put into effect and the signal cavity is blocked, thus disabling the operation of the OPO, the rise in green generated power is significant.

We can model the effect of up-conversion upon the transient dynamics of the device by incorporating an additional term into the rate equation describing the fractional change in pumping field (equation 15) and re-running the model.

$$P_p' = \frac{P_p}{\tau_p} \cdot \left[\frac{n_j \cdot \sigma_j}{1+k} - 1 - \frac{(\sigma_j - 1 - k) \cdot P_s}{1+k} - \delta P \cdot P_p \right] \quad (19)$$

Equation (19) shows the modified pump-field rate equation with the additional term (the last term in the square parenthesis). The parameter δP relates to the magnitude of the SHG effect and it is this parameter which is varied in the model in order to gauge the efficacy of the scheme. This is an empirical value which is determined experimentally by observing the resulting damping time and the drop in down-converted power. We can see that once equation (19) is factored out the rate at which power is lost from the pumping cavity is proportional to δP but to the *square* of P_p . In order to evaluate the impact of the SHG on ICOPO transient dynamics, with particular emphasis on damping time, we re-run the modified numerical model with the same parameters which produced the very long damping time shown in Fig. 13.

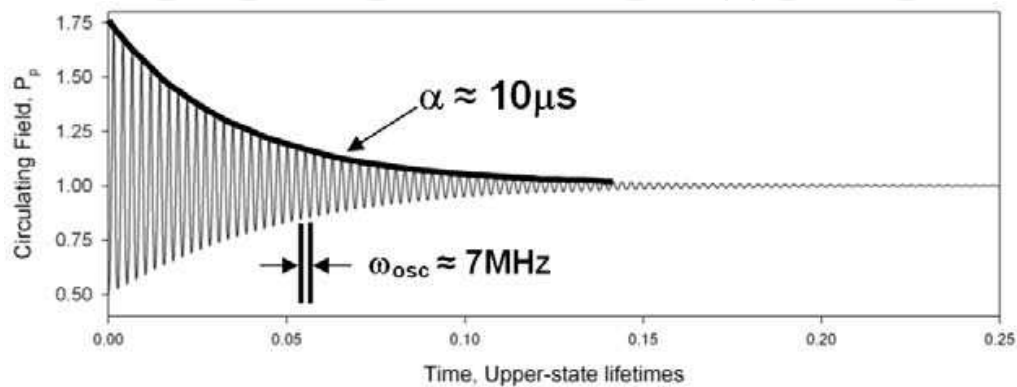


Fig. 17. The modelled effect of SHG on ICOPO transient stability

It is immediately obvious that the inclusion of the SHG crystal has had an enormous impact upon the damping time of the system. As the frequency of the oscillations is governed only by the pump and signal cavity photon decay times, the former of which is not significantly altered by the very low level of SHG, the resulting oscillation frequency is almost the same as the system operating in the absence of up-conversion. We have seen that the laser, operating in the absence of parametric down-conversion, demonstrates a high level of stability when free running and returns to the steady state in about an upper-state lifetime ($\sim 100\mu\text{s}$) once perturbed. The modelled ICOPO, with the SHG stabilisation implemented, demonstrates an even shorter damping time than this – returning to the steady state in only a *tenth* of an upper-state lifetime. It is when the dynamics of the ICOPO with and without the inclusion of the SHG stabilisation are compared that the efficacy of the technique is thrown into particularly sharp relief. A comparison of Fig. 13 and Fig. 17 shows that the inclusion of the SHG crystal within the cavity of the pumping field reduces the damping time by a factor of $\sim 50,000$ – a reduction of well over four orders of magnitude. Clearly, this approach is very effective from the point of view of damping time – but what impact does circulating field lost to frequency up-conversion have upon the total down-converted power? The model is re-run for different levels of δP (i.e. changing the magnitude of the up-conversion effect); the resulting damping time and drop in down-converted power is shown in Fig. 18.

In order for the system to operate with an adequate level of stability (comparable to that of the laser operating in the absence of frequency up- or down-conversion), we require a level of δP which corresponds to a damping time on the order of or less than an upper-state lifetime. This region is indicated by the shaded area in Fig. 18. We can see that a reduction of damping time to between a tenth and a whole upper-state lifetime has only a marginal

penalty in down-converted power – approximately 5% - which is perfectly acceptable when one considers the stability advantage which the SHG process confers.

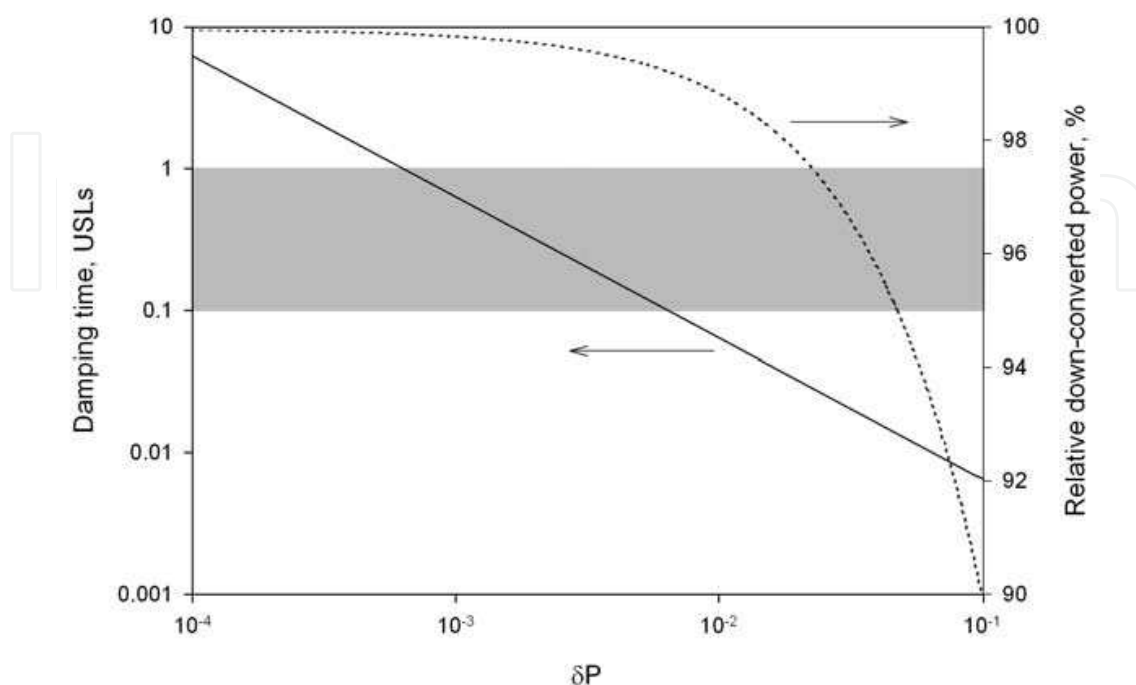


Fig. 18. The impact of increased δP upon damping time and down-converted power. The shaded region corresponds to the zone in which one would prefer to operate.

The strategy outlined above indicates a very promising route to the elimination of relaxation oscillations in the context of the ICOPO – but how well do these modelled results mirror the performance of an actual device? A particular embodiment resulting from the above discussion is illustrated in Fig. 19 (Stothard & Dunn 2009), and is essentially the same design as the system outlined in section 3 (Stothard, Ebrahimzadeh et al. 1998) with the addition of an LBO SHG crystal in the pump field only arm of the device.

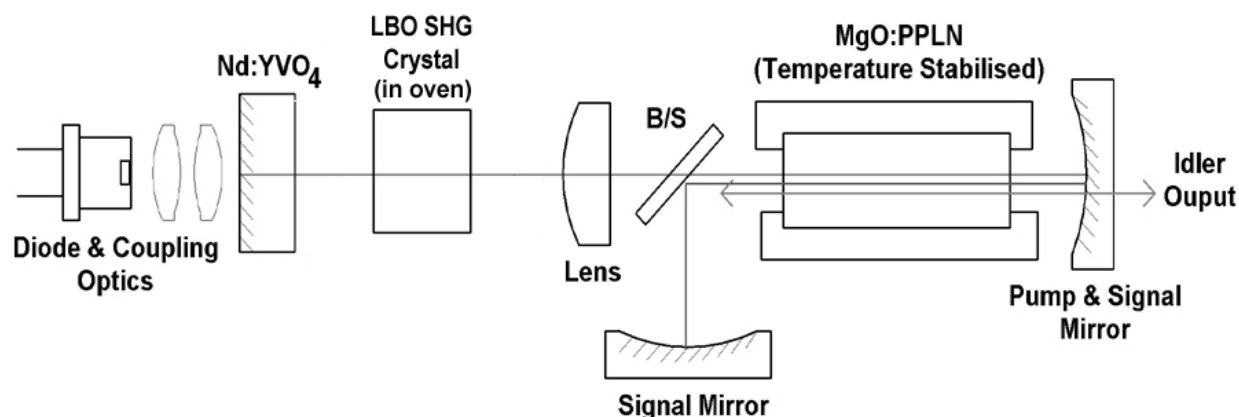


Fig. 19. Experimental configuration of the ICOPO with SHG relaxation oscillation suppression (Stothard & Dunn 2009).

Up-conversion was achieved with an antireflection-coated (for the pump field and its second-harmonic), $2 \times 2 \times 20 \text{mm}^3$ LBO crystal placed in the pump field only section of the

cavity between the Nd:YVO₄ crystal and the intracavity lens. The LBO crystal was placed within a temperature stabilized oven (not shown in the diagram) in order to maintain it at the correct temperature for phase matching. The pump mode was weakly focused in this part of the cavity with a beam diameter of $\sim 300\mu\text{m}$ at the centre of the LBO crystal. Whilst perhaps not the most obvious choice, LBO (as opposed to, say, KTP) was chosen as the doubling crystal as it exhibited type I phase-matching and therefore did not exhibit any bi-refringence into the pumping cavity. This is crucial: such bi-refringence can perturb the polarisation of the circulating pump field and cause the device performance to severely degrade. In addition to this, the efficiency of the SHG, and its impact on the transient stability of the system, could be varied simply by control of the crystal temperature, i.e. without changing the round-trip linear loss of the pump cavity. Finally, the large aperture ($2\times 2\text{mm}^2$) made it easy to accommodate the near-collimated pump mode without the risk of aperturing. A superior, and perhaps more elegant solution, would be to implement a hybrid MgO:PPLN crystal featuring a fanned grating (as shown in Fig. 8 (b)) for rapid control of the signal and idler wavelengths with a non-fanned SHG grating integrated into a small portion at the end of the crystal. Changing the temperature of the crystal would therefore vary (or optimise) the SHG up-conversion and the signal and idler waves would be tuned by translating the crystal laterally through the pumping field. As well as improving the simplicity of the device, such a scheme would also result in four less surfaces for the pump-wave to encounter on each transit of the pump cavity.

In order to gauge the effect of the SHG, regular bursts of relaxation oscillations were induced into the system by rectangular-wave modulation of the diode-laser pumping current. The frequency of the perturbation was 1 kHz with a duty cycle heavily biased towards the diode laser active state. It was important to maintain this very high duty cycle in order to keep the mean thermal load within the Nd:YVO₄ unchanged from the steady-state case. Variations in this parameter are undesirable as it can destabilize or at least modify the stability of the pump cavity by altering the effective radius of curvature of the lens induced into the Nd crystal, thereby changing the threshold conditions of the pump laser and OPO. In order to minimize this effect in the case of external modulation of the diode pump power, the drive current was modulated on a $\sim 90\%$ duty cycle; the mean power delivered to the Nd:YVO₄ crystal thereby changing very little.

The transient dynamics of the system was measured in three modes of operation: with both SHG and the OPO suppressed (in the former by temperature tuning the crystal well away from the phase-matching condition, in the later by blocking the signal cavity); with the OPO operational but no SHG (i.e. operating as a straight-forward ICOPO with no suppression) and finally with operation of both the SHG and parametric process. Measurement of the system response to perturbation from the steady-state in these three regimes was achieved by monitoring the leaking pump field through the signal and idler mirror with a fast photodetector, and the traces obtained under the three operating regimes outlined above are shown in Fig. 20.

As expected, the laser operating in the absence of parametric down-conversion (Fig. 20(a)) exhibits standard relaxation-oscillation behaviour with a damping time of the order of the upper-state lifetime and an oscillation frequency of a few hundred kHz. The anticipated and deleterious impact of OPO operation is shown in Fig. 20(b); both the oscillation frequency and the damping time have risen considerably – although the damping time has only risen by a factor of four or five (and not by the orders-of-magnitude which the model would predict). This is due to parasitic SHG within MgO:PPLN crystal, which cannot be “switched

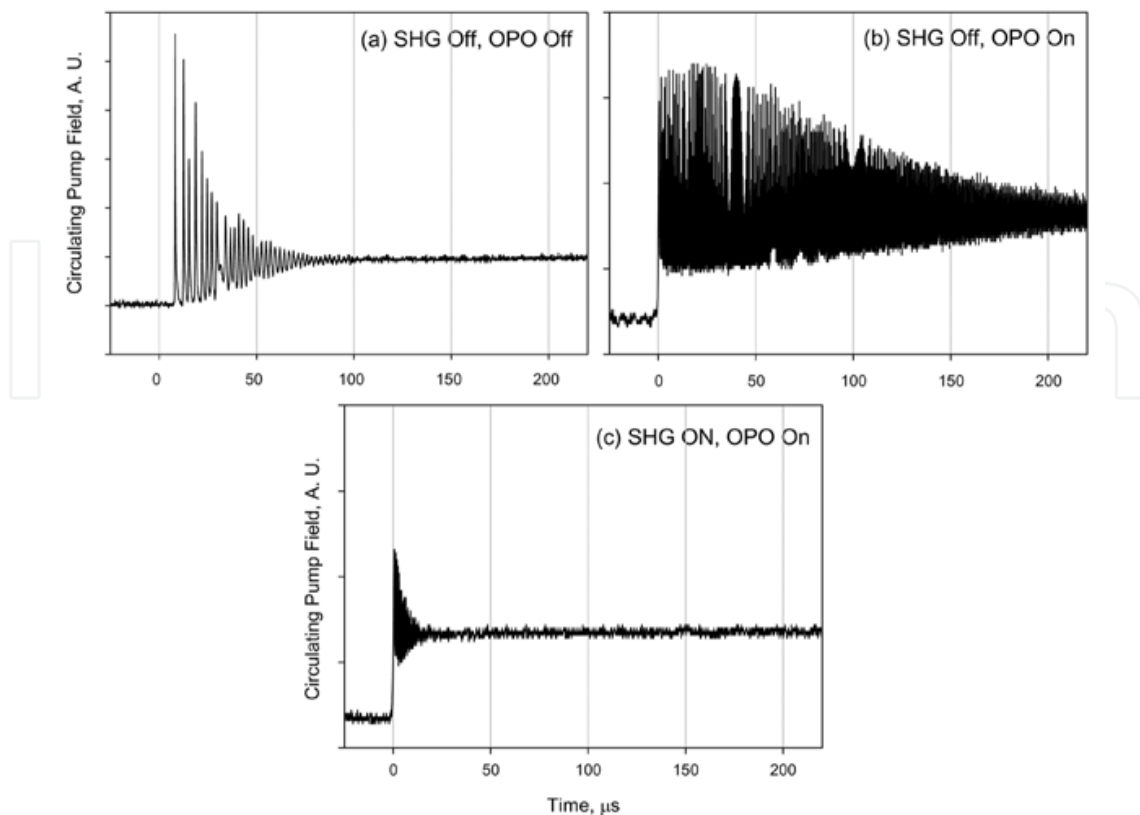


Fig. 20. Transient dynamics of (a) the laser alone, (b) the ICOPO without SHG and (c) the ICOPO with SHG.

off", having a damping effect on the oscillations and also the representative nature of the curve shown in Fig. 20(b) which was very erratic and fluctuated from damping time slightly shorter than that indicated to many 100's μs . Finally, SHG is enabled and the resulting response is shown in Fig. 20(c). Thankfully, the up-conversion has had the intended effect and the damping time of the oscillations has been reduced to even less than that of the simple laser – in this case, about 0.15 upper-state lifetimes ($\sim 15\mu\text{s}$). Although not very clear on the axis scales used in Fig. 20, the oscillation frequency has not been significantly affected by enabling the SHG, as expected. When the modulation of the external pumping diode was ceased, and the device allowed to operate unperturbed in its steady state, it exhibited superb amplitude stability on both the short (100's μs) and long (10's s) timescale, thereby proving the efficacy of this technique.

We can empirically deduce a value of δP resulting from the LBO crystal nonlinearity, interaction length and choice of pump mode focussing by measuring the damping time of the oscillations and comparing them to the curve shown in Fig. 18; doing so indicates a figure of $\delta P \approx 0.005$. Whilst our attention is turned to this figure, and armed with an approximate value of δP , we can also anticipate the drop in down-converted power the SHG oscillation suppression induces – in this case, in the region of 4%. Confirming this drop experimentally is a simple process of measuring the extracted idler power both in the absence and presence of SHG; this is shown as a function of primary diode laser pumping power in Fig. 21. At maximum pumping power, the inclusion of SHG upon the total down-converted power is just $\sim 3\%$; in close agreement with the figure predicted by the model and an entirely acceptable price to pay when one considers the huge improvement in transient stability.

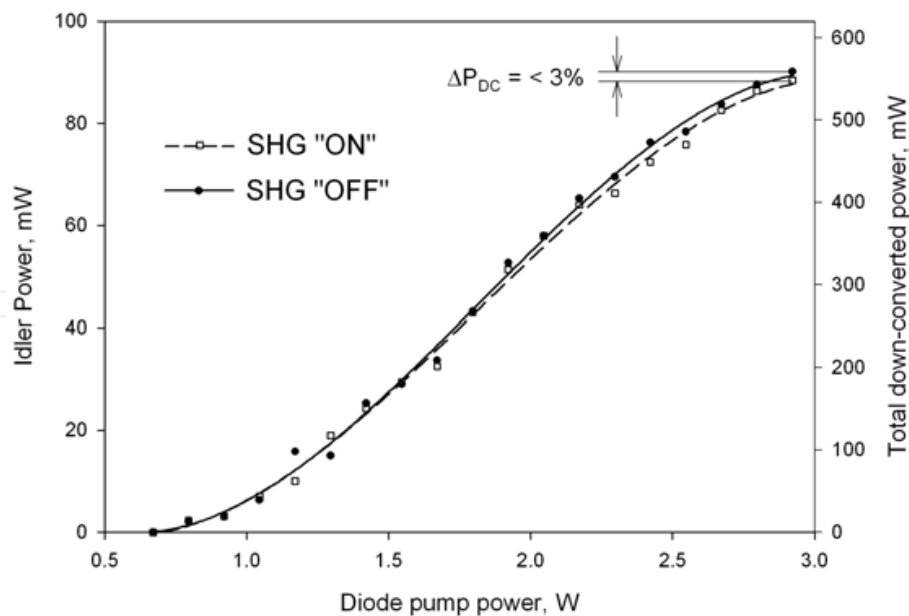


Fig. 21. SHG impact on down-converted power.

5.2 Utilising short upper-state lifetime materials

During our discussion in section 4 we concluded that the susceptibility of the ICOPO to spontaneous bursts of long-lived, high frequency oscillations was a consequence of the long upper-state lifetime exhibited by Nd compared to that of the pump and signal photons within their respective cavities. In this final section we shall discuss the elimination of ICOPO relaxation oscillations by devising a system such that the upper-state and cavity photon lifetimes are comparable by the use of laser gain materials which exhibit very short upper-state lifetimes.

The pioneering early cw-ICOPO work (Colville, Dunn et al. 1997; Turnbull, Edwards et al. 1997; Edwards, Turnbull et al. 1998) was carried out using argon-ion pumped Titanium:Sapphire (Ti:S) lasers, and as such did not experience any problems with the transient instability which have plagued similar systems predicated upon Nd lasers. This is, of course, due to the short upper-state lifetime exhibited by Ti:S of $\sim 3\mu\text{s}$ (approximately two orders of magnitude less than Nd:YAG) in addition to the longer cavity photon lifetimes resulting from the somewhat lengthier cavities used in these systems. Assuming a pump cavity photon lifetime of 20ns and 50ns in the case of a Nd:YAG and Ti:S laser, respectively, then the ratio of the two lifetimes is 60:1 in the case of Ti:S and 10000:1 in the case of Nd:YAG - a very substantial difference which accounts for the absence of relaxation oscillations in these early Ti:S-based devices. A short upper-state lifetime enables the upper-state population to be more responsive to fluctuations in the circulating pump field power and therefore can heavily damp the system even in the presence of the very high frequency oscillations which result from the very high speed power flow from the pump to the signal-wave cavity. ICOPOs based upon Ti:S are in fact excellent optical sources for use in very high resolution spectroscopic applications due to their inherent stability and the ease with which they can be made to operate on a single longitudinal mode; it is only their somewhat cumbersome pumping requirements (i.e. multiwatt, high spatial mode quality green laser radiation and their associated cost and cooling requirements) which has impeded their wide-spread implementation. We therefore require a gain medium which has the combined

advantage of being straight forward to implement in all solid-state, diode pumped designs, as is the case with established gain media such as Nd, whilst exhibiting an upper-state lifetime comparable to or preferably shorter than that of Ti:S.

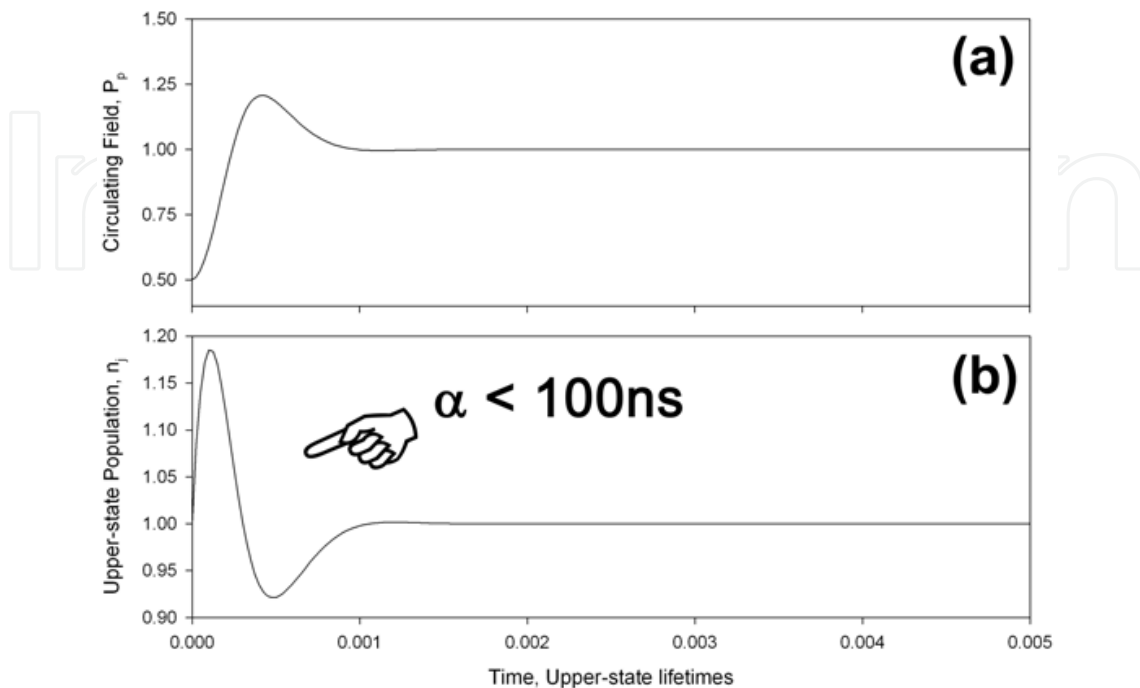


Fig. 22. Modelled transient response of an ICOPO operated internal to a VECSEL. Note that in order to ease comparison with previous figures, the time scale is in units of Nd:YVO₄ upper-state lifetime (100 μ s).

The semiconductor-based gain chips employed in optically-pumped, vertical extended-cavity, surface emitting lasers (VECSELs) are just such media. These materials have received much attention in research laboratories over the last few years due to their numerous meritorious characteristics. Their broad gain bandwidth has made them ideal candidates as a basis for very short pulse width, mode-locked laser systems and the ability to engineer their band-gap rather than rely upon a particular material electronic transition has enabled them to become particularly successful as intracavity SHG sources of visible radiation. For some specific examples of VECSEL devices and an overview of the technology, see (Kuznetsov, Hakimi et al. 1999; Tropper, Foreman et al. 2004; Kim, Cho et al. 2007; Maclean, Kemp et al. 2008); here we shall restrict ourselves to a brief overview of the characteristics pertinent to the realisation of a viable cw-ICOPO device.

Of course, the most important characteristic which VECSEL gain media exhibits in the context of the current discussion is their extremely short upper-state (or, more accurately, carrier) lifetime – on the order of 1ns. This leads to extremely rapid and deep modulation of the upper-state (or carrier) population when the circulating pumping field is perturbed, returning the system to its steady-state in only a few pump cavity transit times. We can confirm this by re-running the model which produced the curves shown in Fig. 13 and Fig. 14 with the same parameters except for a VECSEL-like laser gain medium upper-state lifetime. The resulting exceptionally high damping levels are evident in Fig. 22, where the system returns to the steady-state in just 0.001 Nd:YVO₄ upper-state lifetimes – that is just 100ns. This represents a reduction in damping time of some *five orders of magnitude* when compared to the system

predicated upon Nd. Such performance, if translated into a practical device, would result in excellent amplitude stability, exceeding even that of the Ti:S devices discussed above.

The very thin active region within the VECSEL chip reduces spatial hole burning significantly when compared to the case of the Nd-based laser systems, where absorption depths can be 100's μm . This significantly eases pump-wave longitudinal mode control to the point that single longitudinal mode operation can be realised in standing wave geometries. As the linewidth of the pumping wave is taken up by that of the non-resonant idler, taking steps to operate the pumping cavity in a single frequency makes the VECSEL-based ICOPO an ideal source for very high resolution spectroscopic applications. The second consequence of the very thin gain region is slightly more pragmatic: the elimination of thermally-induced lensing within the pump cavity. From a laser-physicists' perspective, one of the most problematic and vexing parameters one has to evaluate when designing a laser cavity is gauging the magnitude of the thermal lens induced into the gain media. The magnitude of this is sensitive to many inter-related parameters within the system, such as doping concentration, circulating field, extraction efficiency, spot sizes, etc. An incorrect assignation of this parameter renders the position and diameter of the waist within the nonlinear down-conversion crystal ambiguous and can even lead to unexpectedly unstable cavities. It also makes the cavity geometry a function of pumping power and it is often the case that power in / power out curves are skewed by the cavity changing its stability criterion at low pumping levels. All of these issues do not occur when utilising VECSEL gain media as the gain region is too short for any significant thermal lens to form. The essentially two-dimensional geometry of the active region also simplifies mode matching between the circulating pump field and the pumped volume as the divergence of the incident diode-pump radiation has only to spatially overlap with the resonant intracavity mode over a $\sim 1\mu\text{m}$ depth. Lastly, the broad gain-bandwidth of VECSELs, typically 5-10nm, also enable pump tuning of the OPO phase matched condition. Whilst altering the parametric phase-matching condition is the primary tuning mechanism within the system, the added facility of pump-wave tuning is attractive as it can lead to very broad and simple tuning mechanisms when the device is operated under certain circumstances.

An OPO located within the cavity of a VECSEL has recently been demonstrated (Stothard, Hopkins et al. 2009), and is shown in Fig. 23. The cavity is similar in philosophy to that outlined in section 3 except that the gain medium is now a InGaAs-based VECSEL chip and a bi-refringent filter (BRF) is included within the pump wave only section of the cavity. The system was pumped by a fibre-coupled diode laser bar capable of delivering 8.5W onto the surface of the VECSEL. The BRF was included to stop erratic hopping of the pump-field wavelength as the laser tries to avoid the loss introduced into the cavity once the OPO is significantly above threshold.

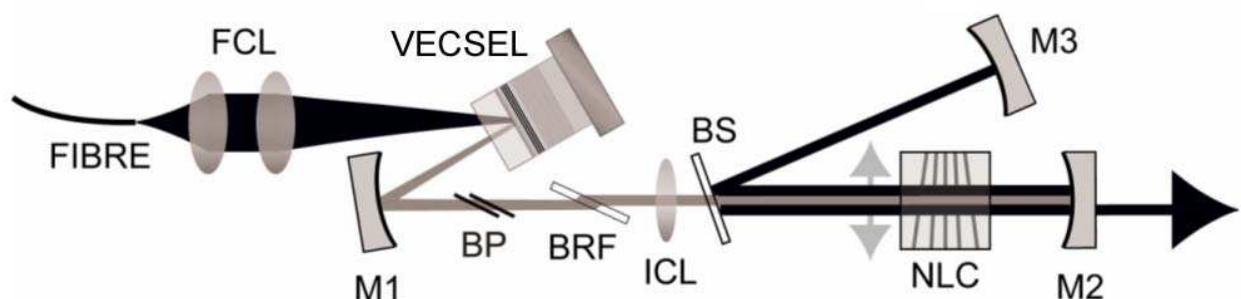


Fig. 23. VECSEL-based cw-ICOPO (Stothard, Hopkins et al. 2009).

This must now be considered as the gain-bandwidth exhibited by VECSEL gain media is so much broader than that of Nd-doped materials. As the BRF is only effective when there is polarisation-dependant loss within the cavity, it is placed into the cavity at Brewster's angle. This however does not induce enough discrimination against unwanted polarisation (and therefore unwanted wavelengths) due to the competing loss of the OPO. Once significantly above threshold the OPO can output-couple significant amounts of power from the circulating pump field into the signal and idler waves. This introduces sufficient round-trip loss such that the laser can operate more effectively by operating against the Brewster surfaces of the BRF alone and rotate its polarisation to a position where the OPO efficiency is substantially diminished. In order to clamp the pump-wave polarisation, and therefore its wavelength, two additional Brewster plates (BP) were included into the cavity. Heat extraction is a significant factor in the successful implementation of VECSEL systems (Kim, Cho et al. 2007; Maclean, Kemp et al. 2008) and so the gain chip was bonded to an uncoated diamond substrate which, due to its very high thermal conductivity, rapidly sinks heat away from the surface of the VECSEL to the copper block into which the assembly was housed. This heat spreader is within the pump cavity and so also acts an étalon for the pump field. A chopping wheel was placed within the pumping cavity in order to investigate the dynamics of the device after disruption from steady-state operation of the device. The resulting behaviour of the circulating field is shown in Fig. 24, where the dynamics of a ICOPO based upon Nd:YVO₄ but with otherwise similar operating parameters is shown for comparison.

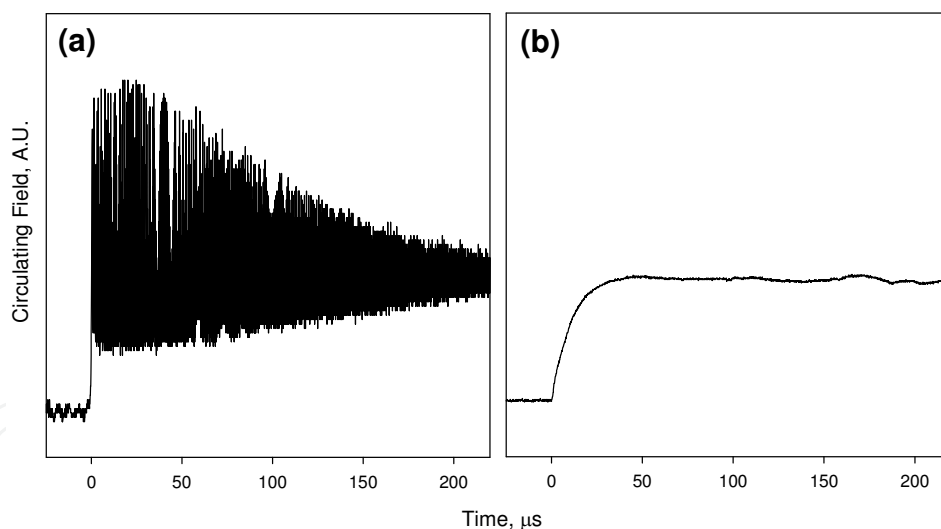


Fig. 24. Recovery transient dynamics of a chopped ICOPO pumped internal to (a) an Nd:YVO₄ and (b) VECSEL laser.

It is immediately obvious that that the VECSEL displays excellent transient stability: there is no trace of oscillatory behaviour at all. The finite rise-time of the trace shown in Fig. 24(b) is simply due to the reveal time of the chopping wheel. When the wheel was removed the pump, signal and idler all exhibited excellent amplitude stability. In order to quantify this free-running stability, the amplitude spectrum of the pump field fluctuations was obtained via the use of an RF spectrum analyser, as shown in Fig. 25 where again a comparable trace obtained from the Nd system is shown for comparison.

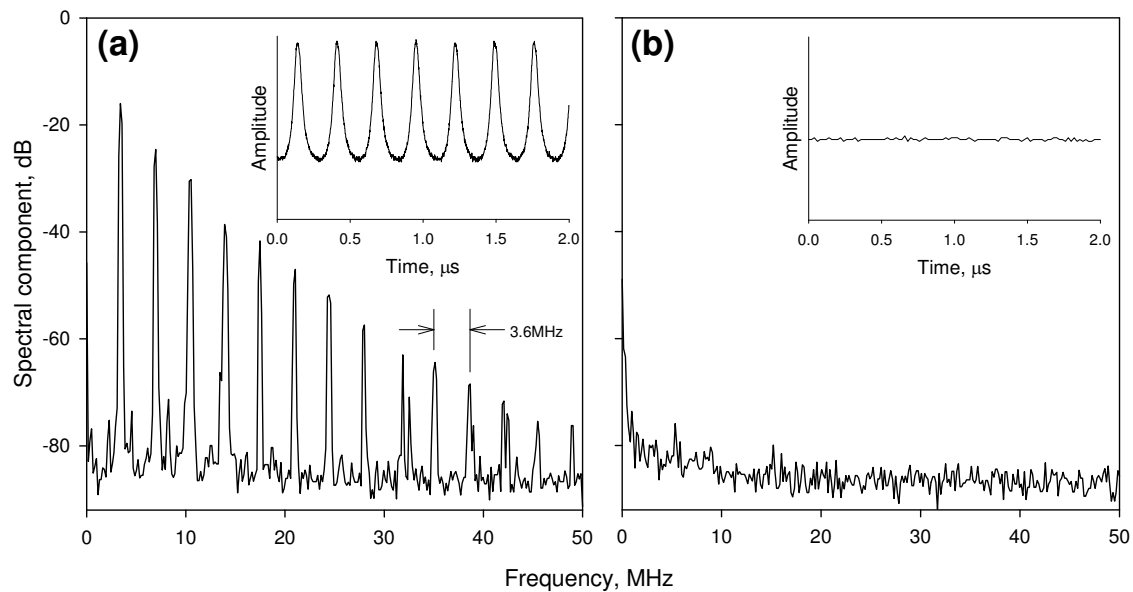


Fig. 25. Amplitude spectrum of the circulating pump field in (a) the Nd:YVO₄- and (b) SDL-based ICSRO. The insert to each panel shows the temporal behaviour of each respective pump field.

The trace shown in Fig. 25 (a), as measured from the Nd-based ICOPO, was obtained during a spontaneous oscillation event as is evident from the characteristic wave form shown in the amplitude-space inset trace. The frequency spectrum shows a large peak at the fundamental oscillation frequency (~ 3.6 MHz) with the higher-order harmonic components tailing off beyond. This is in sharp contrast to the result obtained from the VECSEL system which, as the inset to Fig. 25(b) shows, displayed true cw behaviour. The frequency-space trace only displays spectral content at very low frequencies (not resolvable on the axis scale used in the figure) – a consequence of acousto-mechanical noise within the environment in which the system was operated. Such noise could be easily remedied through the use of established cavity length and amplitude stabilisation techniques, or the implementation of a more robust mechanical design.

We conclude this section by examining the down-converted power characteristics of the device. The considerably higher circulating pump powers available in this device compared to those discussed previously in this chapter, brought about by the enhanced power of the primary pump diode laser, meant that the device could be operated many times above OPO threshold. As we have previously seen, operating the device in this mode results in over-coupling of power from the pump circulating field and hence reduced down-converted powers at maximum primary pump power. In order to optimise the efficiency of the device at full pump power it is therefore necessary to raise the threshold of the OPO such that, for a given laser threshold and primary pumping level, power relation (1) is satisfied. The device could therefore be optimised in one of two regimes: for minimum OPO threshold or maximum obtained power in the extracted idler field at full primary pump power. Both of these cases were demonstrated with the VECSEL ICOPO under discussion, and their down-converted power performance is shown in Fig. 26. In both cases it can be seen that as expected, once the OPO comes above threshold the power in the intracavity circulating pump field clamps at (or near) its OPO threshold value, indicative of a robust optical geometry for the pump-wave and signal-wave cavities. Fig. 26(a) indicates the performance

of the device when optimised for low parametric threshold. Here, laser and OPO threshold are achieved at diode pump powers of 1W and 1.4W respectively. At this latter pumping power a circulating pump field of 3.1W was present within pump cavity.

That OPO threshold is achieved at a power level well within the reach of very modest pumping sources once again shows the great advantage which the intracavity approach bestows. It is clear that in mobile, perhaps battery operated applications where diode-laser primary pump power might be limited to $\sim 3\text{W}$, the device, when optimised in this way, would operate at >2 times threshold delivering an idler power of 30mW. This level is more than adequate for a host of spectroscopic applications. When pumped at the maximum diode-laser pump power of 8.5W, the extracted idler power was 95mW. Hence the calculated total down-converted power, calculated in the previously described manner (equation 13), was 581mW. At this pumping level, the OPO was operating 6 times above threshold and 4.3 times greater than the optimum (in terms of down-conversion efficiency) pumping level of 1.96W, as determined by (1).

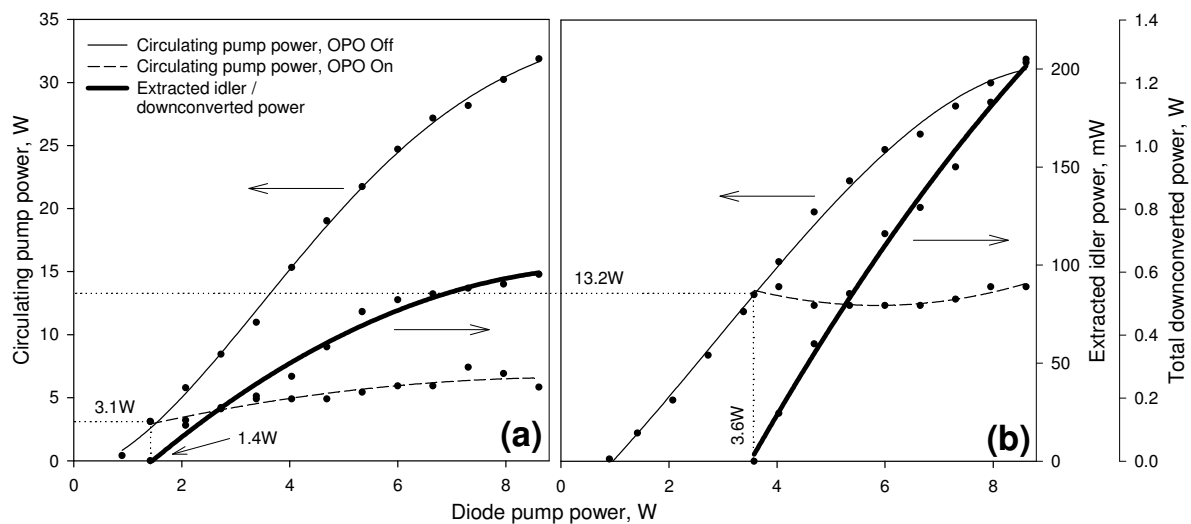


Fig. 26. Downconversion power characteristics of the VECSEL-ICOPO when (a) optimised for lowest threshold and (b) optimised for maximum idler output power. In both cases the threshold of the pump laser occurred at a diode pump power of 1W, and the pump, signal and idler wavelengths were 1050nm, 1600nm and 3055nm respectively.

In order to optimise the down-conversion efficiency of the device when operating at the maximum available primary pumping power, and hence maximise the extracted idler power, it was necessary to increase the threshold of the OPO (but leave the laser threshold unchanged). This was achieved by increasing the mode size of the pump and signal fields within the nonlinear crystal. The resulting curve is shown in Fig. 26(b). The threshold of the OPO, in terms of diode pump power, increased from 1.4W (in the case of the low-threshold device) to 3.6W, at which point the circulating pump field was 13.2W. This threshold pump power is some 700mW greater than the calculated threshold of 2.9W for optimal down-conversion which (1) predicts; possibly a result of non-confocal focusing within the PPLN crystal. The extracted idler power at this pumping level was 205mW, corresponding to a total down-converted power of 1.25W. With the mirror M2 replaced with an optimal output coupler (but the cavity otherwise left unchanged), 1.5W power at the pump wavelength was

obtained. This implies that the 1.25W converted through the parametric process from pump into signal and idler power equates to a down-conversion efficiency of 83.3%.

This system, then, exhibits high-power, broadly tunable output with extremely high efficiency in a compact, robust mechanical design. The synergy of the intracavity technique and emergent semiconductor laser gain media is the culmination of the different topics discussed in this chapter, both in terms of exploiting the benefits of, and managing the issues associated with, the cw-ICOPO technique.

6. Conclusions and outlook

In this chapter we have examined various aspects of the cw-ICOPO in the context of realising low threshold, high efficiency and broadly tunable sources of mid-infrared radiation. We have seen that through an understanding of their origin, steps can be taken in order to either manage or eliminate the relaxation oscillations which have to date barred the cw-ICOPO from use in many of the applications to which it is otherwise ideally suited.

Due to the constraints of space we have unfortunately had to neglect many of the other design aspects of these devices; most notably spectral line narrowing, mode-hop free tuning mechanisms and output-coupling of the resonant down-converted field. It is hoped that armed with the knowledge provided in this chapter, the reader will have the necessary expertise and confidence to design and construct a cw-ICOPO and then be able to use well established laser frequency control and output coupling techniques, which are in the main entirely portable from their use in the parent pump laser to the resonant down-converted wave, in order to adapt their system to meet his or her precise needs.

Neither have we explored the operation of the ICOPO in the Q-switched, pulsed regime: yet another solution to the problem of relaxation oscillations. Here, the long upper-state (storage) lifetime of Nd gain media is turned to our advantage. Whilst the resulting very high intensity peak powers present within the pumping cavity allow the ICOPO to operate over a wider portion of its phase-matching bandwidth, and therefore increases the linewidth of the down converted waves, the system becomes very much less susceptible of the effects of pump and, in particular, signal cavity round-trip loss. This significantly relaxes the tolerance placed upon cavity finesse and therefore allows the tuning bandwidth of the device to be substantially expanded. Through careful gating of the pump cavity Q and taking advantage of high efficiency cavity-dumping of the pump field into signal and idler through the parametric process (Debuisschert, Raffy et. al. 1996), very high repetition rates (100's kHz) are achievable with mean-power efficiencies significantly higher than those normally associated with Q-switched devices (Stoithard, Rae et. al. 2009).

The system we considered in section 5.2 is a particularly exciting stepping stone on our road to realising a truly utile cw-ICOPO ideally suited to high-resolution spectroscopic applications. As we saw, the use of state-of-the-art, semiconductor-based laser gain media eliminates the problems associated with relaxation oscillations, therefore releasing the potential of the cw-ICOPO. By utilising enhanced, ring-resonator designs coupled with existing well-established tuning mechanisms (such as cavity length control, the use of frequency-selective elements, etc.), very broad tunability with single-frequency, mode-hop free tuning over 100's GHz becomes possible. That the gain bandwidth of VECSEL gain media is dictated by its internal structure, rather than a particular electronic transition, opens up the particularly exciting possibility of realising cw devices capable of penetrating much further into the infrared spectral region. This band is currently inaccessible (to cw

devices) due to the limited transparency of established nonlinear materials beyond $\sim 4\mu\text{m}$, therefore mandating the use of semiconductor-based nonlinear optical crystals. These, however, suffer from very poor transparency below $\sim 2\mu\text{m}$. The combination of high power, long wavelength ($>2\mu\text{m}$) circulating pumping fields available within VECSEL-based lasers and very recent advances in low loss periodically-poled semiconductor nonlinear crystals fabricated from GaAs (Schunemann, Pomeranz et al. 2009) could enable the kind of rapid and exciting developments in the field of mid- to deep- infrared parametric devices that PPLN did for shorter wavelength cw devices in the 1990's. Such developments would confirm the continuing importance of ICOPO technology and ensure that, in the absence of radical developments in laser gain media operating directly in the required spectral region, ICOPOs will continue to play an important role in extending the utility and spectral range of laser-based spectroscopic devices for many years to come.

7. References

- Bosenberg, W. R., Drobshoff, A., et al. (1996). 93% pump depletion, 3.5-W continuous-wave, singly resonant optical parametric oscillator. *Optics Letters*, 21(17): 1336-1338.
- Colville, F. G., Dunn, M. D., et al. (1997). Continuous-wave, singly resonant, intracavity parametric oscillator. *Optics Letters*, 22 (2), p75.
- Debuisschert, T., Raffy, J., et al. (1996) Intracavity optical parametric oscillator: study of the dynamics in the pulsed regime. *Journal of the Optical Society of America B - Optical Physics*, 12 (7), pp1569-1587.
- Ebrahimzadeh, M. and Dunn, M. H., (1998). Optical Parametric Oscillators, In: *Handbook of Optics IV - Fiber and Nonlinear Optics*, Bass, M., and Enoch, J. M., (Eds.), pp22.1-22.72, Optical Society of America, ISBN 0-07-136456-0
- Edwards, T. J., Turnbull, G. T. A., et al. (1998). High-power, continuous-wave, singly resonant, intracavity optical parametric oscillator. *Applied Physics Letters*, 72 (13), pp1527-1529.
- Jundt, D. H. (1997). Temperature-dependent Sellmeier equation for the index of refraction n_e in congruent lithium niobate. *Optics Letters*, 22, p1553.
- Kim, J. Y., Cho, S., et al. (2007). Highly efficient green VECSEL with intra-cavity diamond heat spreader. *Electronics Letters*, 43 (2), pp105-107.
- Kuznetsov, M., Hakimi, F., et al. (1999). Design and characteristics of high-power ($> 0.5\text{-W}$ CW) diode-pumped vertical-external-cavity surface-emitting semiconductor lasers with circular TEM₀₀ beams. *IEEE Journal of Selected Topics in Quantum Electronics*, 5 (3), pp561-573.
- Maclean, A. J., Kemp, A. J., et al. (2008). Continuous tuning and efficient intracavity second-harmonic generation in a semiconductor disk laser with an intracavity diamond heatspreader. *IEEE Journal of Quantum Electronics*, 44 (3-4), pp216-225.
- Oshman, M. K. and Harris, S. E., (1968). Theory of Optical Parametric Oscillation Internal to the Laser Cavity. *IEEE Journal of Quantum Electronics*, QE-4 (8), pp491-502.
- Schunemann, P. G., Pomeranz, L. A., et al. (2009). Recent advances in all-epitaxial growth and properties of orientation-patterned gallium arsenide (OP-GaAs). *Conference on Lasers and Electro-Optics*. Baltimore, Optical Society of America, Paper CWJ5.
- Stothard, D. J. M. and Dunn, M. H., (2009). Relaxation-oscillation suppression in intracavity optical parametric oscillators. *Submitted to Optics Express*, September 2009.

- Stothard, D. J. M., Ebrahimzadeh, M., et al. (1998). Low pump threshold, continuous-wave, singly resonant, optical parametric oscillator. *Optics Letters*, 23, p1895.
- Stothard, D. J. M., Rae, C. F., and Dunn, M. H., (2009). An intracavity optical parametric oscillator with very high repetition rate and broad tunability based upon room temperature periodically-poled MgO:LiNbO₃ with fanned grating design. *IEEE Journal of Quantum Electronics*, 45 (3), pp256-263.
- Stothard, D. J. M., Hopkins, J. M., et al. (2009). Stable, continuous-wave, intracavity optical parametric oscillator pumped by a semiconductor disk laser (VECSEL). *Optics Express*, 17 (13), pp10648-10658.
- Tropper, A. C., Foreman H. D., et al. (2004). Vertical-external-cavity semiconductor lasers. *Journal of Physics D - Applied Physics* 37 (9), R75-R85.
- Turnbull, G. A., Dunn, M. H., et al. (1998). Continuous-wave, intracavity optical parametric oscillators: an analysis of power characteristics. *Applied Physics B*, 66, p701.
- Turnbull, G. A., Edwards, T. J., et al. (1997). Continuous-wave singly-resonant intracavity optical parametric oscillator based on periodically-poled LiNbO₃. *Electronics Letters*, 33 (21), pp1817-1818.
- Vodopyanov, K. L., (2003) Pulsed Mid-IR Optical Parametric Oscillators, In: *Solid-state, mid-infrared laser sources*, Sorokina, I. T., Vodopyanov, K. L., (Eds.) p141-174, Springer, ISBN 978-3-540-00621-3

IntechOpen



Advances in Optical and Photonic Devices

Edited by Ki Young Kim

ISBN 978-953-7619-76-3

Hard cover, 352 pages

Publisher InTech

Published online 01, January, 2010

Published in print edition January, 2010

The title of this book, *Advances in Optical and Photonic Devices*, encompasses a broad range of theory and applications which are of interest for diverse classes of optical and photonic devices. Unquestionably, recent successful achievements in modern optical communications and multifunctional systems have been accomplished based on composing “building blocks” of a variety of optical and photonic devices. Thus, the grasp of current trends and needs in device technology would be useful for further development of such a range of relative applications. The book is going to be a collection of contemporary researches and developments of various devices and structures in the area of optics and photonics. It is composed of 17 excellent chapters covering fundamental theory, physical operation mechanisms, fabrication and measurement techniques, and application examples. Besides, it contains comprehensive reviews of recent trends and advancements in the field. First six chapters are especially focused on diverse aspects of recent developments of lasers and related technologies, while the later chapters deal with various optical and photonic devices including waveguides, filters, oscillators, isolators, photodiodes, photomultipliers, microcavities, and so on. Although the book is a collected edition of specific technological issues, I strongly believe that the readers can obtain generous and overall ideas and knowledge of the state-of-the-art technologies in optical and photonic devices. Lastly, special words of thanks should go to all the scientists and engineers who have devoted a great deal of time to writing excellent chapters in this book.

How to reference

In order to correctly reference this scholarly work, feel free to copy and paste the following:

David J. M. Stothard (2010). Practical Continuous-Wave Intracavity Optical Parametric Oscillators, *Advances in Optical and Photonic Devices*, Ki Young Kim (Ed.), ISBN: 978-953-7619-76-3, InTech, Available from: <http://www.intechopen.com/books/advances-in-optical-and-photonic-devices/practical-continuous-wave-intracavity-optical-parametric-oscillators>

INTECH
open science | open minds

InTech Europe

University Campus STeP Ri
Slavka Krautzeka 83/A
51000 Rijeka, Croatia
Phone: +385 (51) 770 447

InTech China

Unit 405, Office Block, Hotel Equatorial Shanghai
No.65, Yan An Road (West), Shanghai, 200040, China
中国上海市延安西路65号上海国际贵都大饭店办公楼405单元
Phone: +86-21-62489820

www.intechopen.com

Fax: +385 (51) 686 166
www.intechopen.com

Fax: +86-21-62489821

IntechOpen

IntechOpen

© 2010 The Author(s). Licensee IntechOpen. This chapter is distributed under the terms of the [Creative Commons Attribution-NonCommercial-ShareAlike-3.0 License](#), which permits use, distribution and reproduction for non-commercial purposes, provided the original is properly cited and derivative works building on this content are distributed under the same license.

IntechOpen

IntechOpen